



ORIGINAL ARTICLE

Differential distribution of phytochemicals in *Scutellariae Radix* and *Scutellariae Amoena Radix* using microscopic mass spectrometry imaging



Lieyan Huang^a, Lixing Nie^{a,1}, Jing Dong^b, Lingwen Yao^a, Shuai Kang^{a,*},
Zhong Dai^a, Feng Wei^a, Shuangcheng Ma^{a,*}

^a National Institutes for Food and Drug Control, National Medical Products Administration, Beijing 102629, China

^b Shimadzu China Innovation Center, Beijing 100020, China

Received 27 October 2022; accepted 12 January 2023

Available online 20 January 2023

KEYWORDS

Mass spectrometry imaging;
Medicinal plants;
Natural compounds;
Traditional Chinese medicine;
Scutellariae Radix;
Scutellariae Amoena Radix

Abstract *Scutellariae Radix*, the root of *Scutellaria baicalensis* Georgi, is widely applied in China for the treatment of fever, ulcer, bronchitis, hepatitis and inflammatory symptoms. *Scutellariae Amoena Radix*, the root of *Scutellaria amoena* C.H. Wright, is often prescribed as the substitute for *Scutellariae Radix*. Up to now, no attempt has been made to unveil and compare the localization of phytochemicals in *Scutellariae Radix* and its succedaneum. This investigation succeeded to look into the differential distribution of natural compounds in *Scutellariae Radix* and *Scutellariae Amoena Radix* using microscopic mass spectrometry imaging. Compounds presenting different distribution modes in two kinds of roots were sorted out, then a quick method for the differentiation between *Scutellariae Radix* and *Scutellariae Amoena Radix* was established. Accumulation sites of baicalin, baicalin, wogonin and wogonoside in *Scutellariae Radix* were also uncovered using microscopic mass spectrometry imaging. Moreover, the application of matrix assisted laser desorption ionization-quadrupole-time of flight mass spectrometry allowed the on-tissue dissociation of major flavonoids. Overall, the utilization of microscopic mass spectrometry imaging and

* Corresponding authors at: National Institutes for Food and Drug Control, Beijing 102629, China.

E-mail addresses: kangshuai@nifdc.org.cn (S. Kang), masc@nifdc.org.cn (S. Ma).

¹ Equal contribution: These authors contributed equally to this work.

Peer review under responsibility of King Saud University.



matrix assisted laser desorption ionization-quadrupole-time of flight mass spectrometry provided a novel perspective for the discovery of natural compounds within medicinal plants.

© 2023 Published by Elsevier B.V. on behalf of King Saud University. This is an open access article under the CC BY-NC-ND license (<http://creativecommons.org/licenses/by-nc-nd/4.0/>).

1. Introduction

Plants of the *Scutellaria* L. genus (the Lamiaceae family) are perennial herbs represented by around 360 species. Most of the *Scutellaria* species are widely spread in European, North American and Eastern Asian regions (Karimov and Botirov, 2017). A number of *Scutellaria* plants are utilized for clinical use since ancient times. For example, *Scutellariae Radix* (SR), the root of *Scutellaria baicalensis* Georgi, is widely used to treat fever, ulcer, bronchitis, hepatitis and inflammatory symptoms (Liu et al., 2009). It has been proved by modern pharmacological research that the extracts of SR possessed anti-tumor, antiviral, anti-microbial, anti-oxidative and neuroprotective bioactivities (Wang et al., 2018). SR is now included officially in Chinese Pharmacopoeia (Chinese Pharmacopoeia Commission, 2020). During the past decades, different classes of phytochemicals were isolated from SR, including flavonoids, lignins, amides, and phenylethanoid glycosides (Liu et al., 2019; Qiao et al., 2016). Flavonoids are the major bioactive components of SR (Ji et al., 2015). Baicalein, wogonin, baicalin and wogonoside are four well-known flavonoids extracted from the SR (Zhao et al., 2016), which have been proved to exert anti-tumor activities (Liu et al., 2016; Huynh et al., 2017; Tao et al., 2018; Sun et al., 2016). Among the four major flavonoids, baicalin is selected as the chemical marker of SR in Chinese Pharmacopoeia (Chinese Pharmacopoeia Commission, 2020).

In Southwest China, the root of *Scutellaria amoena* C.H. Wright, namely, *Scutellariae Amoena Radix* (SAR), is often prescribed as the substitute for SR. It was illustrated in a previous study that the natural constituents in SAR were quite different from that in SR (Zhang et al., 2007). Over the years, many attempts have been made to look into the difference of phytochemicals between the two *Scutellaria* species. In 2016, an investigation was carried out to differentiate SR and SAR using liquid chromatography coupled with mass spectrometry (LC-MS) (Ling et al., 2016).

When illustrating the chemical compositions of a medicinal plant, conventional analytical methods such as LC-MS usually require that the samples be homogenized before analysis, thus the spatial information of natural constituents is lost during sample preparation step. Besides, when natural compounds were extracted from the crude drugs, ultra-sonication or heating reflux procedures may easily lead to the decomposition or loss of components (Husain et al., 2020). To overcome the drawbacks of the previous analytical methods, a new technique named mass spectrometry imaging (MSI) has been adopted to explore the material basis of medicinal plants.

MSI is a frontier analytical method which allows direct visualization of endogenous metabolites in native tissues. Over the decades, MSI has been applied to various kinds of fields, such as pathology (Chung et al., 2022), pharmacy (Schulz et al., 2019), cancer research (McDonnell et al., 2017) and plant science (Sturtevant et al., 2015). The application of MSI in photochemistry puts forward the exploration of natural compounds in medicinal plants (Huang et al., 2022b). For the MSI analysis of plant metabolomes, matrix assisted laser desorption ionization mass spectrometry imaging (MALDI-MSI) and desorption electrospray ionization mass spectrometry imaging (DESI-MSI) are two commonly applied techniques (Huang et al., 2022b; Bjarnholt et al., 2014). Compared with conventional analytical tools, MSI requires less or even no sample pretreatment, thus not only saves time and labor, but also avoids the possible loss of constituents during extraction or purification process (Husain et al., 2020). In an MSI analytical task, various classes of natural compounds could be simultaneously detected by MSI (Kuo et al., 2019). Accumulation sites of natural components uncovered by MSI could

serve as a guidance for high-efficiency extraction of active components (Feng et al., 2014). Additionally, the localization patterns of phytochemicals illustrated by MSI could also provide new perspectives on the biosynthesis of pharmaceutical constituents in medicinal plants (Freitas et al., 2019; Marques et al., 2014). More recently, comparative analysis of spatial information of natural constituents in different plant samples were carried out under the method of MSI (Duan et al., 2022; Huang et al., 2022a).

Up to now, there have been a few investigations attempting to map out the distribution of secondary metabolites in SR using MSI (Feng et al., 2014; Pramanik et al., 2019). However, the reproducibility of component distribution across duplicate or multiple SR samples were not mentioned in previous studies. In order to draw a more accurate and universal conclusion of compound distribution in SR samples, it was necessary to conduct MSI analysis towards SR samples collected from different habitats. In our work, SR samples were collected from four different provinces in China, therefore the results of component distribution in SR were more convincing. The spatial distribution of phytochemicals in SAR was also explored in our investigation, which has not been studied in any previous research.

Using microscopic MSI, this study illustrated the differential distribution of metabolomes in SR and SAR. Visualization of components in roots collected from the two species was achieved using matrix assisted laser desorption ionization-quadrupole-time of flight mass spectrometry (MALDI-Q-TOF-MS). Localization patterns of detected chemicals in the roots of two *Scutellaria* species were compared, providing information for the quick differentiation from SR and SAR. Particularly, four pharmaceutically important flavonoids in SR and SAR were accurately identified by on-tissue tandem mass spectrometry analysis.

2. Materials and methods

2.1. Plant materials

Scutellariae Radix (SR), Huang-Qin in Chinese, is the root of *Scutellaria baicalensis* Georgi. *Scutellariae Amoena Radix* (SAR), Dian-Huang-Qin in Chinese, is the root of *Scutellaria amoena* C.H. Wright. SAR and SR samples were collected from different habitats in China. Samples of SAR (Sample A-B) were bought from the local market of Chinese materia medica in Yunnan, China. Samples of SR (Sample C-F) were bought from the local markets of Chinese materia medica in four provinces of China. Sample C was bought from Hebei, Sample D was bought from Neimenggu, Sample E was bought from Shanxi, and Sample F was bought from Shandong. The origin of Samples A-B was authenticated as the root of *Scutellaria amoena* C.H. Wright by Associate Professor Shuai Kang in accordance with the Yunnan Standard of Chinese Materia Medica (Medical Products Administration of Yunnan Province, 2005). The origin of Samples C-F was authenticated as the root of *Scutellaria baicalensis* Georgi by Associate Professor Shuai Kang in accordance with the Chinese Pharmacopoeia (Chinese Pharmacopoeia Commission, 2020). For future reference, the voucher specimens (Samples A-F) were deposited in National Institutes for Food and Drug Control, Beijing, PR China.

Table 1 Putative identification results of phytochemicals detected from *Scutellariae Amoena Radix* and/or *Scutellariae Radix*.

No.	Compound name	Formula	Adduct ion	Theoretical m/z	Measured m/z	Mass error (ppm)	Ref
1	(2 <i>R</i> ,3 <i>R</i>)-3,5,7,2',6'-Pentahydroxyflavanone/ <i>Trans</i> -5,7,2',6'-tetrahydroxyflavanonol/ 3,6,7,2',6'-Pentahydroxyflavanonol/ DihydroviscidulinI	C ₁₅ H ₁₂ O ₇	M + Na	327.0475	327.0473	0.64	(Ji et al., 2015; Takagi et al., 1981; Tomimori et al., 1981)
2	(2 <i>S</i>)-5,6,3',4'-Tetrahydroxyflavanone/7- <i>O</i> -β- <i>D</i> -glucuronide/(2 <i>S</i>)-5,8,3',4'- Tetrahydroxyflavanone-7- <i>O</i> -β- <i>D</i> - glucuronide	C ₂₁ H ₂₀ O ₁₃	M + Na	503.0796	503.0799	0.54	(Liu et al., 2011)
3	(2 <i>S</i>)-5,7,4'-Trihydroxy-6- methoxyflavanone/(2 <i>S</i>)-7,2',6'-Trihydroxy- 5-methoxyflavanone/2,6,2',4'-Tetrahydroxy- 6'-methoxychalcone/5,7,4'-Trihydroxy-6- methoxyflavanone/5,7,4'-Trihydroxy-8- methoxyflavanone	C ₁₆ H ₁₄ O ₆	M + Na	325.0683	325.0680	1.17	(Takagi et al., 1980; Tomimori et al., 1984; Zhou et al., 2000)
4	(2 <i>S</i>)-5-Hydroxy-6-methoxyflavanone-7- <i>O</i> -β- <i>D</i> -glucoside	C ₂₂ H ₂₄ O ₁₀	M + Na	471.1262	471.1268	1.17	(Miyaiichi et al., 1995)
5	3-Caffeoylquinic acid/Chlorogenic acid	C ₁₆ H ₁₈ O ₉	M + Na	377.0843	377.0826	4.56	(Wang et al., 2009; Xiong et al., 2022)
6	4- <i>O</i> -β- <i>D</i> -glucosyl- <i>trans</i> - <i>p</i> -coumaric acid/4- <i>O</i> -β- <i>D</i> -glucosyl- <i>cis</i> - <i>p</i> -coumaric acid	C ₁₅ H ₁₈ O ₈	M + Na	349.0894	349.0892	0.57	(Liu et al., 2009)
7	5-(2-hydroxyethyl)-2-methoxyphenol	C ₉ H ₁₂ O ₃	M + K	207.0424	207.0426	1.16	(Syrjänen et al., 2000)
8	5,2',5'-Trihydroxy-6,7,8-trimethoxyflavone	C ₁₈ H ₁₆ O ₈	M + K	399.0482	399.0467	3.71	(Tomimori et al., 1984)
9	5,6,7-Trihydroxy-4'-methoxyflavone/5,7,2'- Trihydroxy-6'-methoxyflavone/5,7,2'- Trihydroxy-6-methoxyflavone/5,7,2'- Trihydroxy-8-methoxyflavone/5,7,4'- Trihydroxy-8-methoxyflavone/5,8,2'- Trihydroxy-7-methoxyflavone/TenaxinIII/ 5,7,4'-Trihydroxy-6-methoxyflavone/4'- Hydroxywogonin/5,7,6'-Trihydroxy-2'- methoxyflavone/Scutevulin /5,8,2'- Trihydroxy-7-methoxyflavone	C ₁₆ H ₁₂ O ₆	M + K	339.0271	339.0265	1.68	(Takagi et al., 1980; Tomimori et al., 1983; Tomimori et al., 1984; Xiao et al., 2003)
10	5,6'-Dihydroxy-6,7,8-trimethoxyflavone-2'- <i>O</i> -β- <i>D</i> -glucoside	C ₂₄ H ₂₆ O ₁₃	M + Na	545.1266	545.1274	1.47	(Ishimaru et al., 1995)
11	5,6'-Dihydroxy-7,8-dimethoxyflavone-2'- <i>O</i> - β- <i>D</i> -glucoside/5,6'-Dihydroxy-6,7- dimethoxyflavone-2'- <i>O</i> -β- <i>D</i> -glucoside	C ₂₃ H ₂₄ O ₁₂	M + K	531.0905	531.0899	1.13	(Miyaiichi et al., 1995; Ishimaru et al., 1995)
12	5,6-Dihydroxy-7-methoxyflavone/ Methoxybaicalein/Oroxylin A/Wogonin/5, 8-Dihydroxy-7-methoxyflavone/Genkwanin	C ₁₆ H ₁₂ O ₅	M + K	323.0322	323.0309	4.06	(Takagi et al., 1980; Popova et al., 1973; Wang et al., 2016)
13	5,7,2'-Trihydroxy-6,8-dimethoxyflavone/ 5,8,2'-Trihydroxy-6,7-dimethoxyflavone/ 5,7,6'-Trihydroxy-8,2'-dimethoxyflavone/ 5,7,2'-trihydroxy-8,6'-dimethoxyflavone/ ViscidulinII/5,8,2'-Trihydroxy-6,7- dimethoxyflavone/5,6',2'-Trihydroxy-7,8- methoxyflavone	C ₁₇ H ₁₄ O ₇	M + K	369.0377	369.0384	1.76	(Takagi et al., 1980; Tomimori et al., 1984)
14	5,7-Dihydroxy-6,8-dimethoxyflavone/5, 8- Dihydroxy-6,7-dimethoxyflavone/ SkullcapflavoneI/5, 8-Dihydroxy-6,7- dimethoxyflavone	C ₁₇ H ₁₄ O ₆	M + K	353.0428	353.0425	0.85	(Takagi et al., 1980; Ma et al., 2013; Takido et al., 1979)
15	5,7-Dihydroxy-6,8-dimethoxyflavone-7- <i>O</i> - glucuronide	C ₂₃ H ₂₂ O ₁₂	M + K	529.0748	529.0724	4.59	(Liu et al., 2012)
16	6'-Hydroxy-5,6,7,8,2'-pentamethoxyflavone	C ₂₀ H ₂₀ O ₈	M + H	389.1231	389.1249	4.73	(Han et al., 2010)
17	Adipic acid dioctyl ester	C ₂₂ H ₄₂ O ₄	M + K	409.272	409.2705	3.76	(Yang et al., 1999)
18	Amoenin B	C ₂₂ H ₂₂ O ₁₂	M + Na	501.1004	501.0982	4.33	(Zhou et al., 2000)
19	Amoenin C/(2 <i>S</i>)-5,7,6'- Trihydroxyflavanone-2'- <i>O</i> -β- <i>D</i> -glucoside	C ₂₁ H ₂₂ O ₁₁	M + Na	473.1054	473.1045	1.90	(Zhou et al., 2000)
20	Amoenin D/Amoenin E	C ₂₁ H ₂₂ O ₁₂	M + Na	489.1004	489.0986	3.76	(Zhou et al., 2000)

(continued on next page)

Table 1 (continued)

No.	Compound name	Formula	Adduct ion	Theoretical m/z	Measured m/z	Mass error (ppm)	Ref
21	Apigenin-7-O- β -D-glucoside/5,6-Dihydroxy-7-O-glucosideflavone/Baicalein-7-O- β -D-glucoside	C ₂₁ H ₂₀ O ₁₀	M + Na	455.0949	455.0965	3.60	(Tomimori et al., 1984; Ma et al., 2013)
22	Arginine	C ₆ H ₁₄ N ₄ O ₂	M + K	213.0755	213.0761	2.68	(Nie et al., 2021)
23	Baicalein/Norwogonin/Apigenin/2'-Hydroxychrysin	C ₁₅ H ₁₀ O ₅	M + H	271.0601	271.0590	4.06	(Tomimori et al., 1984; Popova et al., 1973; Ma et al., 2013)
24	Baicalin/Norwogonin-7-O- β -D-glucuronide/Apigenin-7-O- β -D-glucuronide	C ₂₁ H ₁₈ O ₁₁	M + K	485.0486	485.0478	1.59	(Ji et al., 2015; Ishimaru et al., 1995; Cha et al., 2006)
25	Chrysin	C ₁₅ H ₁₀ O ₄	M + K	293.0216	293.0208	2.83	(Takagi et al., 1980)
26	Chrysin-6-C- β -D-glucoside-8-C- α -L-arabinopyranoside/Chrysin-6-C- α -L-arabinopyranoside-8-C- β -D-glucoside/Chrysin-6-C- β -L-arabinopyranoside-8-C- β -D-glucoside/Chrysin-6-C- β -D-glucoside-8-C- β -L-arabinopyranoside/Chrysin-6-C- β -arabinofuranoside-8-C- β -D-glucoside/Chrysin-6-C- β -D-glucoside-8-C- β -L-arabinofuranoside/Chrysin-3-C- α -arabinopyranoside-8-C- β -D-glucoside	C ₂₆ H ₂₈ O ₁₃	M + H	549.1603	549.1591	2.19	(Zhou et al., 1997; Lin et al., 2013)
27	Chrysin-7-O- β -D-glucuronide	C ₂₁ H ₁₈ O ₁₀	M + K	469.0537	469.0533	0.77	(Ma et al., 2013)
28	Chrysin-8-C- β -D-glucoside/Chrysin-6-C- β -D-glucoside	C ₂₁ H ₂₀ O ₉	M + H	417.118	417.1171	2.09	(Miyachi et al. 1994)
29	Darendoside A	C ₁₉ H ₂₈ O ₁₁	M + K	471.1269	471.1268	0.32	(Miyachi et al., 1995)
30	Ferulic acid methyl ester	C ₁₁ H ₁₂ O ₄	M + K	247.0373	247.0380	2.75	(Xu et al. 2016)
31	Fructose/Galactose/Glucose/Mannose/Inositol	C ₆ H ₁₂ O ₆	M + K	219.0271	219.0271	0.05	(Kim et al. 2014)
32	Isocarhamidin/Carthamidin/(+)-Eriodictyol/(2S)-5,7,2',6'-Tetrahydroxyflavanone/5,7,2',6'-Tetrahydroxyflavone/Carthamidin/Isocarhamidin	C ₁₅ H ₁₂ O ₆	M + Na	311.0526	311.0517	2.99	(Takido et al. 1976; Kubo et al. 1981; Zheng et al. 1998)
33	Isoscutellarein-8-O- β -D-glucuronide	C ₂₄ H ₂₄ O ₁₂	M + Na	527.116	527.1170	1.97	(Nagai et al. 1998)
34	Jatrorrhizine	C ₂₀ H ₂₀ NO ₄	M + Na	361.1285	361.1268	4.79	(Deng et al. 2008)
35	Lamivudine	C ₈ H ₁₁ N ₃ O ₃ S	M + K	268.0158	268.0160	0.56	(Kenney et al. 2000)
36	p-Coumaric acid	C ₉ H ₈ O ₃	M + H	165.0546	165.0545	0.42	(Kim et al. 2014)
37	phthalic acid decyl hexyl ester/phthalic acid bis(2-ethyhexyl) ester	C ₂₄ H ₃₈ O ₄	M + K	429.2407	429.2402	1.28	(Yang et al., 1999)
38	phthalic acid isodecyl ester/phthalic acid decyl octyl ester	C ₂₆ H ₄₂ O ₄	M + K	457.272	457.2721	0.18	(Yang et al., 1999)
39	Quinic acid	C ₇ H ₁₂ O ₆	M + K	231.0271	231.0260	4.67	(Kim et al. 2014)
40	Raffinose	C ₁₈ H ₃₂ O ₁₆	M + K	543.1328	543.1309	3.57	(Kim et al. 2014)
41	Salicylic acid/p-Hydroxybenzoic acid	C ₇ H ₆ O ₃	M + H	139.039	139.0394	3.16	(Kim et al. 2014)
42	Salidroside	C ₁₄ H ₂₀ O ₇	M + K	339.0846	339.0850	1.30	(Zhou et al., 1997)
43	Scutellarein/Isoscutellarein/5,7,2',5'-Tetrahydroxyflavone/5,7,2',6'-Tetrahydroxyflavone	C ₁₅ H ₁₀ O ₆	M + K	325.0115	325.0114	0.26	(Tomimori et al., 1984; Ma et al., 2013; Zhang et al. 1994)
44	SkullcapflavoneII/5,4'-Dihydroxy-6,7,3',5'-tetramethoxyflavone/5,2'-Dihydroxy-6,7,8,3'-tetramethoxyflavone/5,7-Dihydroxy-8,2',3',6'-tetramethoxyflavone/6,6'-Dihydroxy-5,7,8,2'-tetramethoxyflavone	C ₁₉ H ₁₈ O ₈	M + K	413.0639	413.0631	1.84	(Ishimaru et al., 1995; Ma et al., 2013; Long et al. 2015; Nishikawa et al. 1999)
45	Sucrose/Cellobiose/Trehalose	C ₁₂ H ₂₂ O ₁₁	M + K	381.0799	381.0793	1.52	(Kim et al. 2014)
46	TenaxinI/Rivularin	C ₁₈ H ₁₆ O ₇	M + K	383.0533	383.0519	3.79	(Tomimori et al., 1983; Zhou et al., 1997)
47	Tryptophan	C ₁₁ H ₁₂ N ₂ O ₂	M + K	243.0536	243.0532	1.52	(Kim et al. 2014)
48	Vanillic acid	C ₈ H ₈ O ₄	M + K	207.006	207.0061	0.29	(Kim et al. 2014)
49	ViscidulinI/2',3,5,6',7-Pentahydroxyflavone	C ₁₅ H ₁₀ O ₇	M + K	341.0064	341.0059	1.55	(Tomimori et al., 1984)

Table 1 (continued)

No.	Compound name	Formula	Adduct ion	Theoretical m/z	Measured m/z	Mass error (ppm)	Ref
50	Wogonoside/Oroxylin A-7- <i>O</i> - β - <i>D</i> -glucuronide	C ₂₂ H ₂₀ O ₁₁	M + K	499.0643	499.0630	2.69	(Ishimaru et al., 1995; Zhang et al. 1997)
51	ViscidulinIII-6'- <i>O</i> - β - <i>D</i> -glucoside/ ViscidulinIII-2'- <i>O</i> - β - <i>D</i> -glucopyranoside	C ₂₃ H ₂₄ O ₁₃	M + K	547.0854	547.0849	0.88	(Takagi et al., 1980; Zhou et al., 1997)

2.2. Chemicals and reagents

2-Nitrophenol (NPG), acetonitrile, trifluoroacetic acid, and gelatin were purchased from Sigma-Aldrich (St. Louis, MO, United States). Reference standards of baicalin, wogonin, baicalin and wogonoside were purchased from Shanghai Standard Technology Co. (Shanghai, China). Ultra-pure water was obtained from a Milli-Q water purification system (Millipore, Bedford, MA, United States). Optimum cutting temperature compound (OCT) was supplied by Leica (Nussloch, Germany).

2.3. Sample preparation

Roots harvested from different habitats were cut into pieces with length within 2 cm using a blade, and the small pieces were embedded in 0.09 g/ml gelatin solution and fast-frozen at -80°C for 20 min. The frozen samples were axially fixed to a cryomicrotome (Leica, Nussloch, Germany) and were sectioned into 30 μm slices. Afterwards, the thin slices of fresh tissues were thaw-mounted onto an indium tin oxide-coated (ITO) glass slide (Matsunami Glass, Osaka, Japan).

Reference solutions of baicalin, wogonin, baicalin and wogonoside were prepared at a concentration of 100 mg/ml in 80 % acetonitrile respectively. Then 1 μl of the reference solution of each flavonoid was dropped onto the surface of a steel plate using a pipette.

Prior to MSI analysis, transverse sections on the ITO glass slide and dried droplets on the steel plate were deposited with NPG matrix. The NPG solution was prepared at a concentration of 10 mg/ml in 80 % acetonitrile containing 0.1 % trifluoroacetic acid. The matrix solution was uniformly sprayed to the sample surface using an automatic sprayer system iMLayer AERO (Shimadzu, Kyoto, Japan). Twenty layers of matrix solution were successively sprayed onto the sample surface at a flow rate of 60 $\mu\text{l}/\text{min}$.

2.4. Mass spectrometry imaging analysis

MSI analysis was conducted using the iMScope QT instrument (Shimadzu, Kyoto, Japan). The Imaging MS Solution Ver.2 software was used to carry out the on-line control of iMScope QT instrument. Optical images of sample sections were captured using stereo microscope with FusionOptics (Leica, Nussloch, Germany). Then, the sample holder was aligned and the alignment information was registered in the instrument. Before data acquisition, acquisition areas were defined according to the botanical structures displayed in optical images. Data

points locating within the acquisition areas were analyzed by a high-performance time-of-flight mass spectrometer equipped with an atmospheric pressure chamber for matrix assisted laser desorption ionization (AP-MALDI) source. Accumulated 500 laser shots per pixel were acquired using a diode-pumped 355 nm Nd:YAG laser, with a laser repetition frequency of 1000 Hz. The diameter of laser spots was set at 25 μm , while the laser intensity was kept at 76.5 (arbitrary unit in iMScope). The spatial resolution of acquired data was set at 50 μm . Mass spectra were generated in positive ion detection mode, and the mass range was m/z 100–550. The detector voltage was set at 2.20 kV for all samples.

2.5. On-tissue tandem mass spectrometry analysis

On-tissue tandem mass spectrometry was performed using iMScope QT instrument (Shimadzu, Kyoto, Japan). Tandem mass data was directly acquired from the transverse sections of SR deposited with selected matrix. Ions at m/z 271.0601 (baicalin, $[\text{M} + \text{H}]^+$), 285.0757 (wogonin, $[\text{M} + \text{H}]^+$), 447.0922 (baicalin, $[\text{M} + \text{H}]^+$) and 461.1078 (wogonoside, $[\text{M} + \text{H}]^+$) were selected as the precursors. Collision energy was set at 35 ± 15 V. Tandem mass spectrometry analysis of reference standards was also carried out, serving as a reference for the fragmentation patterns of the analytes.

2.6. Data analysis

The software ImageReveal MS was employed to process and visualize MSI data. In image registration step, the optical image of a sample was aligned with the mass image. Then regions of interest (ROI) were mapped out according to the optical images. Mass data collected from pixels within the ROIs were calculated and processed. Afterwards, ion images of different chemicals were reconstructed. Putative identification of detected compounds was carried out basing on the accurate m/z value with reference to previous literatures.

3. Results

3.1. In situ profiling of phytochemicals in *Scutellariae Radix* and *Scutellariae Amoena Radix*

According to the basic knowledge of plant development, successive increments of secondary xylem and phloem result in the diametric growth of root. In hence, average mass spectrum generated from a 90° sector of the transverse section should be capable of representing the chemical composition of the intact

sample section. Mass data collected from each coordinate within the defined area were calculated into an average spectrum of the sample. The representative average mass spectra of SAR and SR samples were displayed in Fig. 1.

Mass peaks of six average mass spectra generated from SR and SAR samples were extracted and then combined into a template. Later on, mass images of components contained in the template were constructed. By comparing the ion image with corresponding optical image, the accumulation site of a target compound could be readily obtained. Putative identification results of detected compounds were listed in Table 1.

3.2. On-tissue tandem mass spectrometry analysis of major flavonoids in *Scutellariae Radix* and *Scutellariae Amoena Radix*

Collision induced dissociation usually brings about C-ring cleavage of flavonoids, producing characteristic fragments of flavonoids. When tandem mass spectrometry is performed, MS/MS spectra of protonated flavonoids tend to yield fragments contained either intact A ring or intact B ring, namely $^{1,3}A^+$, $^{1,3}B^+$, $^{0,2}B^+$ and $^{0,4}B^+$ (Wolfender et al., 2000). The general rules of nomenclature for product ions generated from flavonoids were illustrated in Fig. 2 (Cuyckens and Claeys, 2004; Ma et al., 1997). Structures of four major flavonoids were presented in Fig. 3. Tandem mass spectra generated from the precursor ions of four flavonoids in SR tissues were displayed in Fig. 4. Meanwhile, tandem mass spectrometry analysis of reference standards of four major flavonoids was also performed, the results of which were shown in Fig. 5.

Baicalein was trihydroxylated on A ring, the characteristic ions of which were the $^{1,3}A^+$ fragment and $^{1,3}B^+$ fragment. In tandem mass spectrum generated from the cross section of SR displayed in Fig. 4, product ions of protonated baicalein was detected at m/z 169.0110 attributed to the $^{1,3}A^+$ fragment and m/z 103.0531 attributed to the $^{1,3}B^+$ fragment. The ion at m/z 123.0070 was assigned to the $^{0,4}A^+$ fragment. Another product ion resulted from neutral loss of H_2O was found at m/z 253.0496.

For the structure of wogonin, a methoxy group and two hydroxyl groups were distributed on different positions of A ring. The loss of a methoxy group from wogonin gave rise to the product ion at m/z 270.0518. Fragment at m/z 168.0048 was assigned to $(^{1,3}A^+-CH_3)$ ion dissociated from wogonin. Continuous loss of CO brought about the presence of $(^{1,3}A^+-CH_3-CO)$ at m/z 140.0098.

Baicalin and wogonoside are the glucuronides of baicalein and wogonin, respectively. The cleavage of glucosidic bond led to the neutral loss of a glucuronic acid, producing the Y_0^+ ion. The informative Y_0^+ fragment of baicalin showed presence at m/z 271.0597, and Y_0^+ fragment of wogonoside was detected at m/z 285.0756.

In order to confirm the fragmentation patterns of baicalein, wogonin, baicalin and wogonoside, reference standards of these four flavonoids were also analyzed using on-tissue tandem mass spectrometry. Characteristic fragments of the four reference standards were found to be in consistency with the fragments detected from the flavonoids on sample surface. For instance, the $^{1,2}A^+$ and $^{0,4}A^+$ fragments of baicalein were also detected at m/z 169.0110 and m/z 123.0069, matching with the fragments observed in tandem spectrum that was directly acquired from the transverse section of SR.

3.3. Differential distribution patterns of phytochemicals in *Scutellariae Radix* and *Scutellariae Amoena Radix*

Phytochemicals presenting various distribution patterns in SAR and SR were classified into four different groups. The detailed information of distribution pattern was listed in Table 2. The optical images of each sample were shown in Fig. 6. Typical mass images representing each distribution pattern were displayed under each category. The color band attached to each mass image offered a reference for the evaluation of relative abundance of visualized components in sample tissues. In a mass image, as the color changed in the order of white, red, yellow, green, blue and black, the content of an extracted ion presented a descending trend. Therefore, the distribution and relative concentration of metabolites in

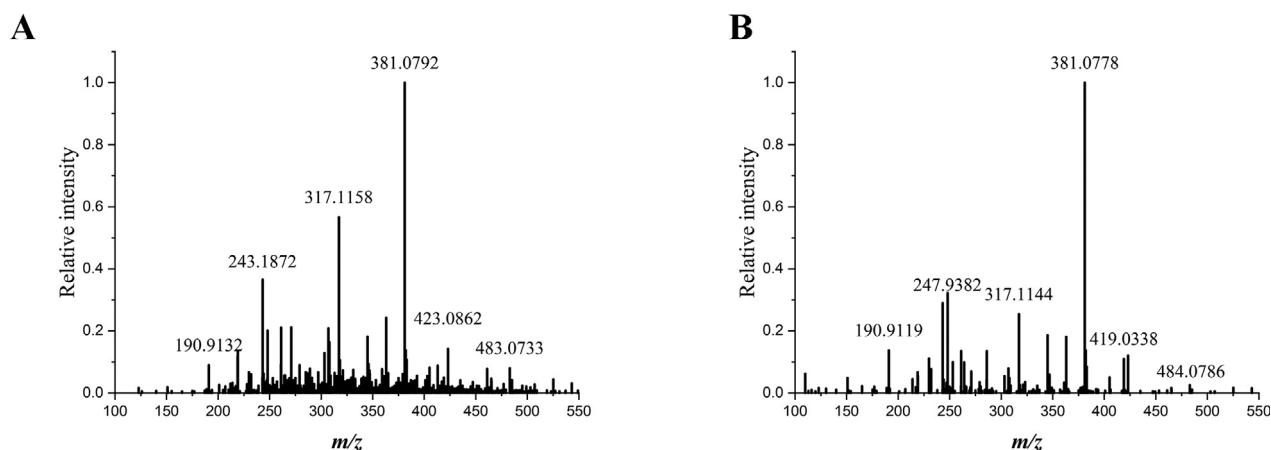


Fig. 1 Typical average mass spectra of *Scutellariae Amoena Radix* (A) and *Scutellariae Radix* (B). Mass spectra were generated at mass range of m/z 100–550 using MALDI-Q-TOF-MS.

Table 2 Phytochemicals of four distribution patterns detected using MALDI-MSI.

Distribution pattern	Compound name
1	Unknown (<i>m/z</i> 433.3448) Unknown (<i>m/z</i> 461.3752) Unknown (<i>m/z</i> 477.3728)
2	Unknown (<i>m/z</i> 385.0347) 5,2',5'-Trihydroxy-6,7,8-trimethoxyflavone Unknown (<i>m/z</i> 400.0450) Unknown (<i>m/z</i> 407.9619) Unknown (<i>m/z</i> 412.0695) SkullcapflavoneII/5,4'-Dihydroxy-6,7,3',5'-tetramethoxyflavone/5,2'-Dihydroxy-6,7,8,3'-tetramethoxyflavone/5,7-Dihydroxy-8,2',3',6'-tetramethoxyflavone/6,6'-Dihydroxy-5,7,8,2'-tetramethoxyflavone Unknown (<i>m/z</i> 421.9798) Unknown (<i>m/z</i> 429.0534) Unknown (<i>m/z</i> 451.0341) 5,6'-Dihydroxy-7,8-dimethoxyflavone-2'- <i>O</i> - β - <i>D</i> -glucoside/5,6'-Dihydroxy-6,7-dimethoxyflavone 2'- <i>O</i> - β - <i>D</i> -glucoside ViscidulinIII -6'- <i>O</i> - β - <i>D</i> -glucoside/ViscidulinIII -2'- <i>O</i> - β - <i>D</i> -glucopyranoside
3	5,6-Dihydroxy-7-methoxyflavone /Methoxybaicalein/Oroxylin A/Wogonin/5,8-Dihydroxy-7-methoxyflavone/Genkwanin 5,6,7-Trihydroxy-4'-methoxyflavone/5,7,2'-Trihydroxy-6'-methoxyflavone/5,7,2'-Trihydroxy-6-methoxyflavone/5,8,2'-Trihydroxy-7-methoxyflavone/5,7,4'-Trihydroxy-6-methoxyflavone/5,7,6'-Trihydroxy-2'-methoxyflavone/TenaxinII/4'-Hydroxywogonin/Scutevulin 5,7,2'-Trihydroxy-6,8-dimethoxyflavone/5,8,2'-Trihydroxy-6,7-dimethoxyflavone/5,7,6'-Trihydroxy-8,2'-dimethoxyflavone/ 5,7,2'-trihydroxy-8,6'-dimethoxyflavone/ViscidulinII/5,8,2'-Trihydroxy-6,7-dimethoxyflavone/5,6',2'-Trihydroxy-7,8-methoxyflavone TenaxinI/Rivularin Amoenin D/Amoenin E
4	(2 <i>S</i>)-5,6,3',4'-Tetrahydroxyflavanone-7- <i>O</i> - β - <i>D</i> -glucuronide/(2 <i>S</i>)-5,8,3',4'-Tetrahydroxyflavanone-7- <i>O</i> - β - <i>D</i> -glucuronide Baicalein/Norwogonin/Apigenin/2'-Hydroxychrysin (2 <i>R</i> ,3 <i>R</i>)-3,5,7,2',6'-Pentahydroxyflavanone/ <i>Trans</i> -5,7,2',6'-tetrahydroxyflavanonol/3,6,7,2',6'-Pentahydroxyflavanonol/ DihydroviscidulinI 2,5,6'-Trihydroxy-7,8-dimethoxyflavone-2'- <i>O</i> -glucuronide 3-Caffeoylquinic acid/Chlorogenic acid 4- <i>O</i> - β - <i>D</i> -glucosyl- <i>trans-p</i> -coumaric acid/4- <i>O</i> - β - <i>D</i> -glucosyl- <i>cis-p</i> -coumaric acid 5,7-Dihydroxy-6,8-dimethoxyflavone-7- <i>O</i> -glucuronide Apigenin-7- <i>O</i> - β - <i>D</i> -glucoside/5,6-Dihydroxy-7- <i>O</i> -glucosideflavone/Baicalein-7- <i>O</i> - β - <i>D</i> -glucoside Baicalin/Norwogonin-7- <i>O</i> - β - <i>D</i> -glucuronide/Apigenin-7- <i>O</i> - β - <i>D</i> -glucuronide Chrysin-7- <i>O</i> - β - <i>D</i> -glucuronide Chrysin-8- <i>C</i> - β - <i>D</i> -glucoside/Chrysin-6- <i>C</i> - β - <i>D</i> -glucoside Isoscutellarein-8- <i>O</i> - β - <i>D</i> -glucuronide Raffinose Scutellarein/Isoscutellarein/5,7,2',5'-Tetrahydroxyflavone/5,7,2',6'-Tetrahydroxyflavone Sucrose/Cellobiose/Trehalose ViscidulinI/2',3,5,6',7-Pentahydroxyflavone Wogonoside/Oroxylin A-7- <i>O</i> - β - <i>D</i> -glucuronide

plant tissues were intuitively revealed in the form of colorful images.

3.3.1. Pattern 1

Phytochemicals with *m/z* values of 433.3448, 461.3752 and 477.3728 were found to show a preferential occurrence in the corks of six samples. The corks here referred to not only corks in normal periderms, but also corks in the abnormal structures, including the interxylary cork and rhytidome.

Interxylary cork and rhytidome were not found in two samples of SAR. As can be seen from Fig. 7, chemicals of Pattern 1 presented strong signals in the form of circular curves along the outer periderm of six samples. Besides, in Samples B-E, the intense signals marked out parallel curves along the border of root sections, indicating that a duplicated structure might be

developed during root growth. Using Zeiss Axio Scan.Z1 automatic digital slide scanning system, double layers of corks were observed in Samples B-E, and a typical scanning image was provided in Fig. 8. As a result, the presence of rhytidome in these samples was confirmed. For Sample F collected from Neimenggu, intense signals were found not only around the border of root section, but also at the edge of interxylary cork.

3.3.2. Pattern 2

Phytochemicals of Pattern 2 showed different distribution features in SAR and SR (see Fig. 7). Mass signals of detected metabolites appeared especially high intensities in the cork regions of SR, including the interxylary cork and sequent corks of rhytidome. In contrast, these chemicals presented no preferential accumulation in the corks of SAR. Such phenom-

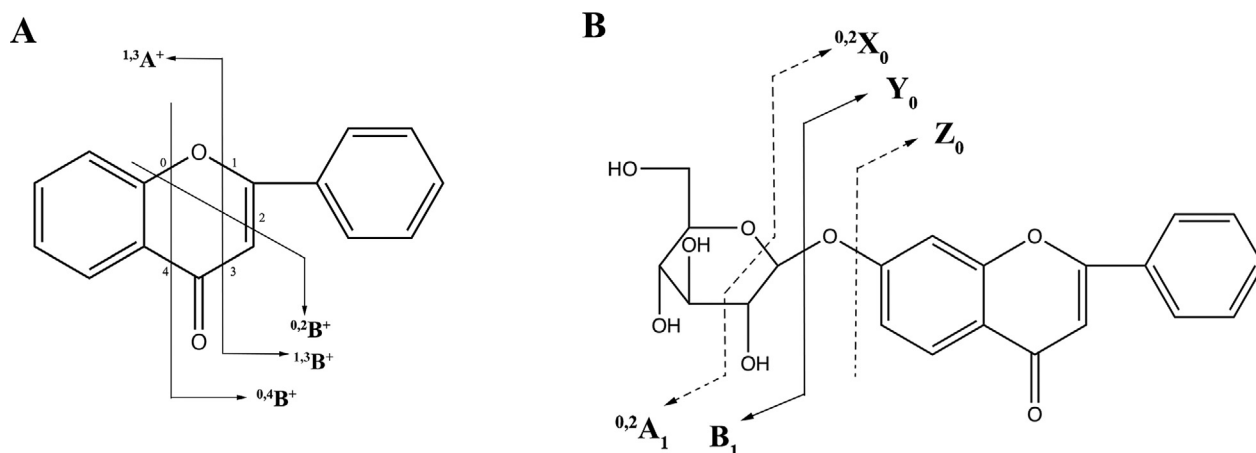


Fig. 2 Nomenclature and diagnostic product ions of protonated flavonoid (A) and flavonoid glycoside (B).

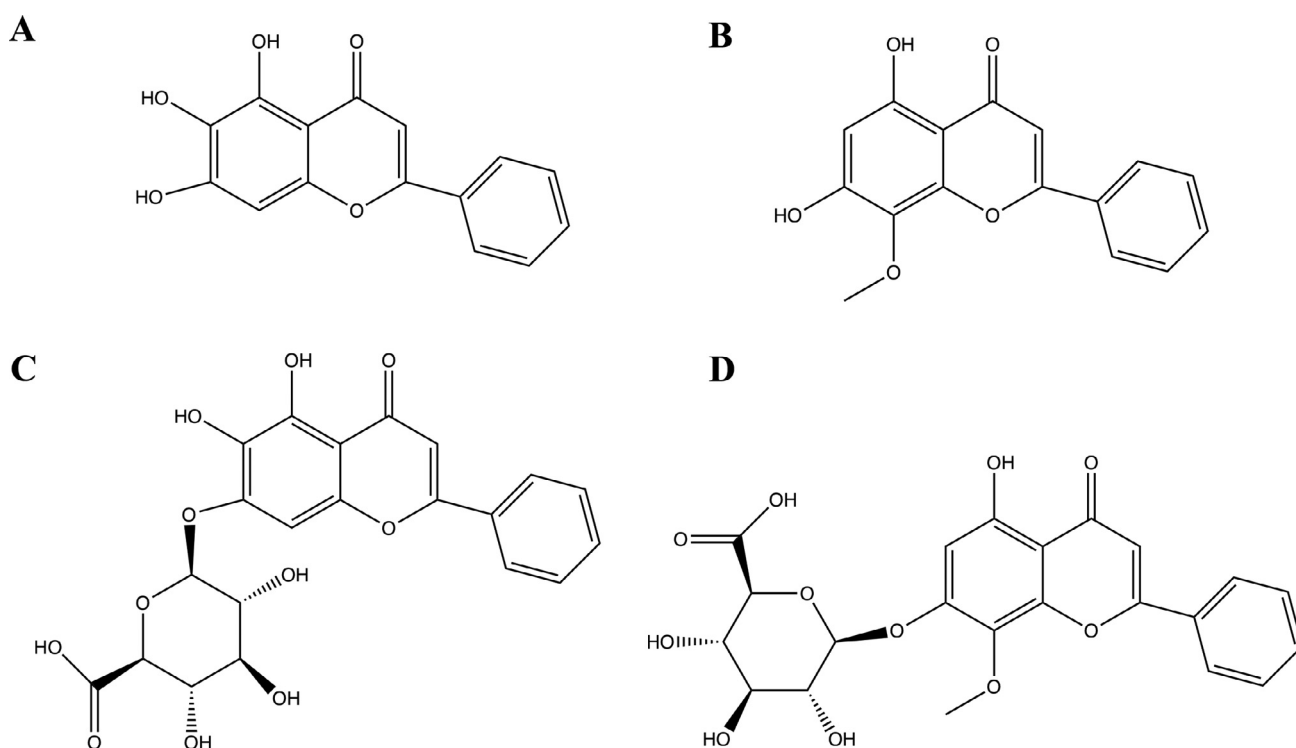


Fig. 3 Chemical structures of four major components, including baicalein (A), wogonin (B), baicalin (C) and wogonoside (D).

ena illustrated by mass images could be utilized to quickly differentiate between SAR and SR. As listed in Table 2, a number of components were included in the classification of Pattern 2, some were identified by comparing the measured m/z values with theoretical m/z values of known compounds, while the others remained unknown.

3.3.3. Pattern 3

Phytochemicals of Pattern 3 followed a similar distribution mode to Pattern 2, the slight difference was that these chemicals were observed to show an intense signal in the dead phloem or dead xylem associated with the development of abnormal structures. As displayed in Fig. 7, especially high

intensity of detected compounds was found in dead phloem tissues in between the successive corks of rhytidome or in dead xylem tissues within the interxylary cork of SR. However, these chemicals presented a uniform distribution mode in the root sections of SAR.

3.3.4. Pattern 4

As illustrated in Fig. 7, phytochemicals falling into this category were observed to be widely distributed in the root sections of six samples, showing no apparent distribution difference. A group of natural compounds, including knowns and unknowns, were found to show a homogenous distribution in both SAR and SR.

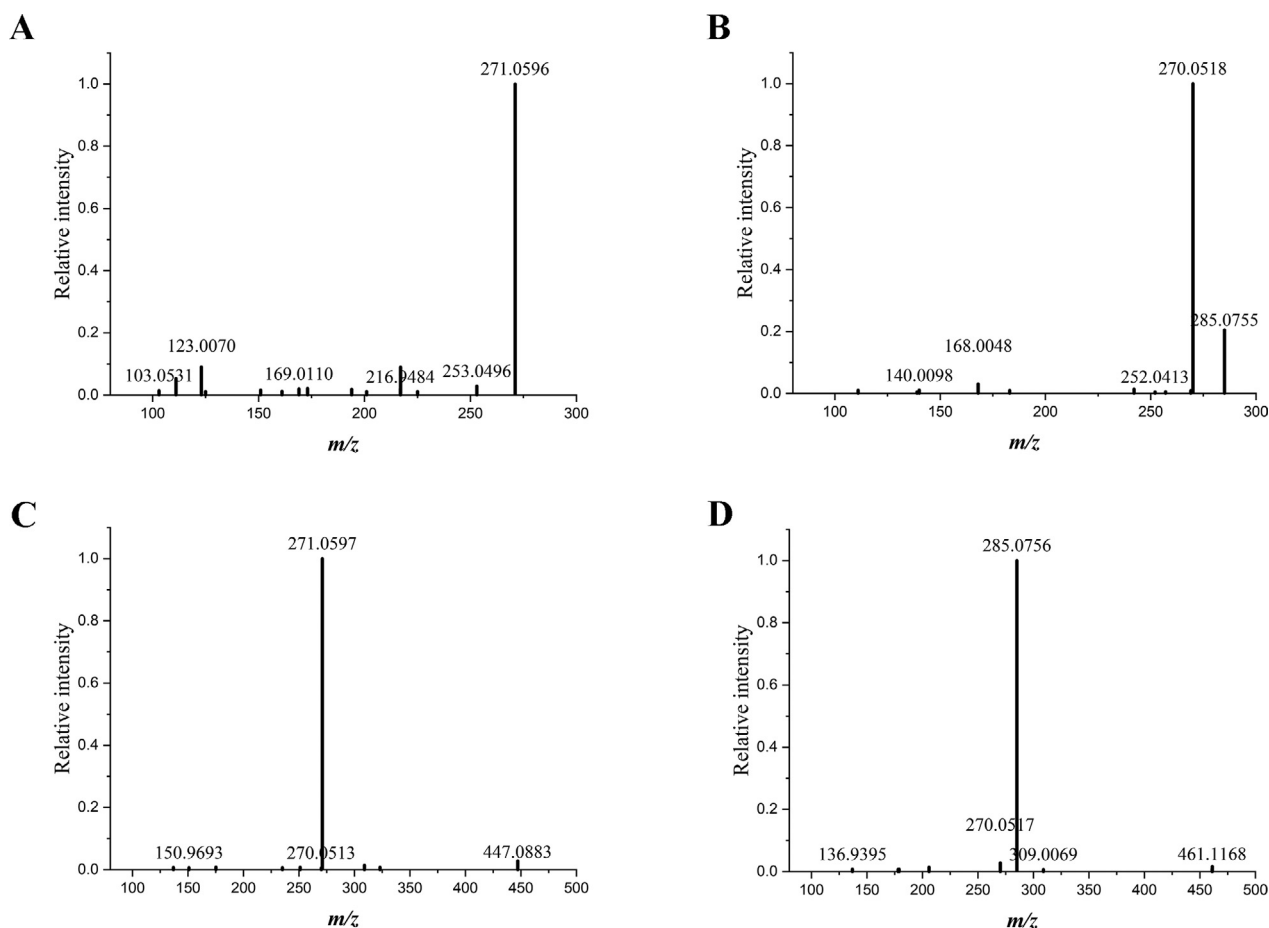


Fig. 4 Tandem mass spectra of baicalein (A), wogonin (B), baicalin (C) and wogonoside (D) in *Scutellariae Radix*. The spectra were directly acquired from the transverse section of *Scutellariae Radix*.

3.4. Visualization of four major flavonoids in *Scutellariae Radix* and *Scutellariae Amoena Radix*

Baicalein, wogonin, baicalin and wogonoside are four pharmaceutically important flavonoids in SR. As shown in Fig. 9, baicalein and wogonin were widely distributed in the whole transverse section, with an extremely high intensity along the edge of rhytidome or interxylary cork. For the distribution of wogonoside and baicalin, no apparent accumulation in specific area was observed. The localization of two glucuronides appeared a quite uniform pattern within the root tissues.

4. Discussion

4.1. Optimization of experimental conditions

Three matrices, including 2,5-dihydroxybenzoic acid (DHB), α -cyano-4-hydroxycinnamic acid (CHCA) and 2-nitrophenol (NPG), were tested for the MALDI-Q-TOF-MS detection of natural compounds in SAR and SR. Different matrix solution was mixed with the reference solution of baicalein, baicalin, wogonin and wogonoside. The mixed solution was deposited onto a steel plate and then ana-

lyzed using MALDI-Q-TOF-MS. Mass spectra generated from droplets containing different matrix solution and reference solution were compared with each other. The intensities of protonated flavonoids showed highest intensity when NPG was used as the matrix. As a result, NPG was selected as the optimum matrix for MSI analysis of SR and SAR.

The parameters of laser setup were optimized basing on the test firing function of Imaging MS Solution. The laser energy and laser diameter were tested by performing imaging acquisition at different regions of root sections. According to the signal intensity of mass acquisition, the optimum diameter of laser spots was set at 25 μm , and laser intensity was kept at 76.5 (arbitrary unit in iMScope).

As for tandem mass spectrometry, optimization of collision energy was carried out by analyzing the reference solution that was deposited on a steel plate. The collision energy set at 35 ± 15 V brought about the presence of abundant fragments, and was selected as the appropriate collision energy for tandem mass spectrometry analysis of four major flavonoids.

4.2. In situ profiling of phytochemicals in *Scutellariae Radix* and *Scutellariae Amoena Radix*

Though MSI visualization of a target compound might be interfered by its possible isomers, the imaging results were still

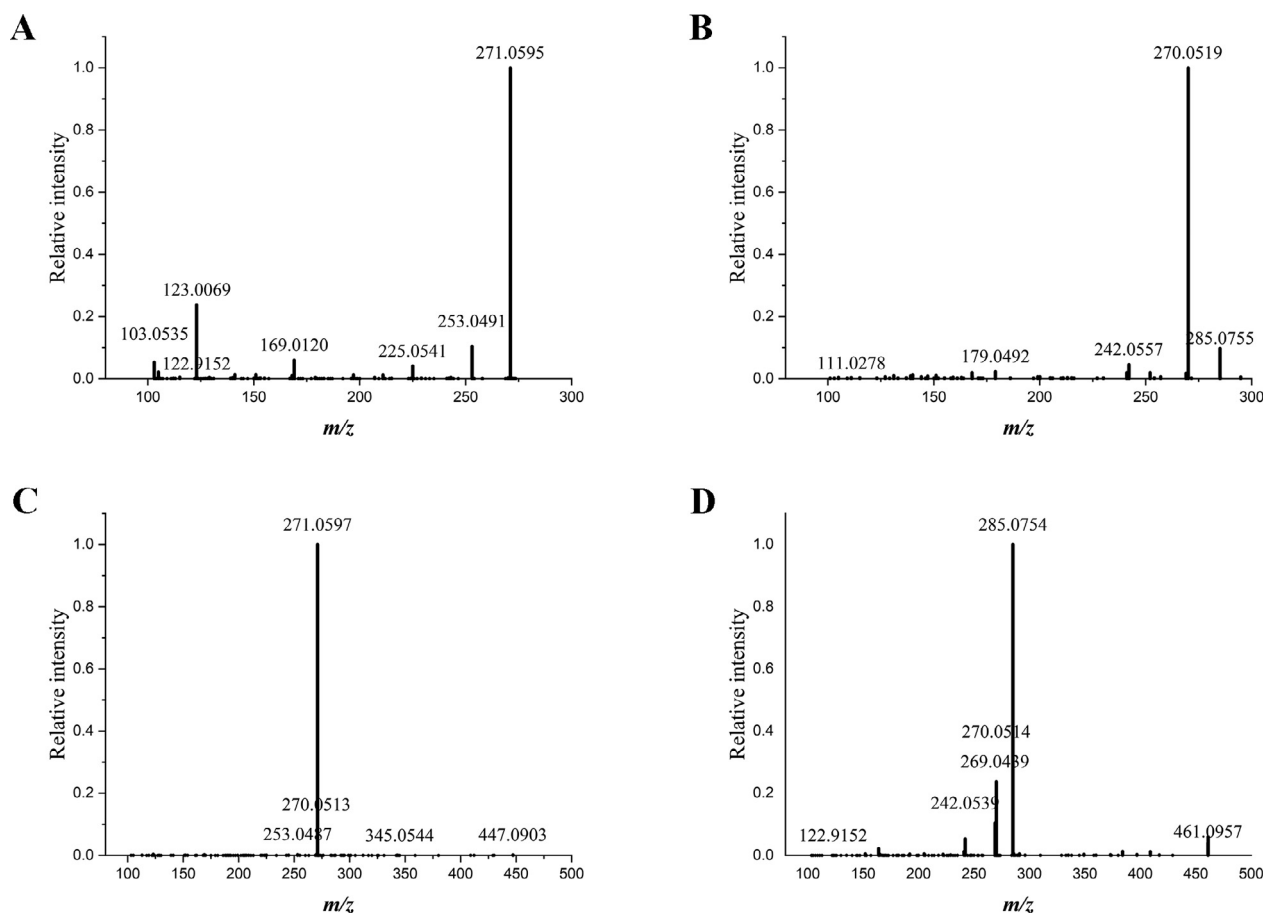


Fig. 5 Tandem mass spectra generated from the reference standards of baicalein (A), wogonin (B), baicalin (C) and wogonoside (D).

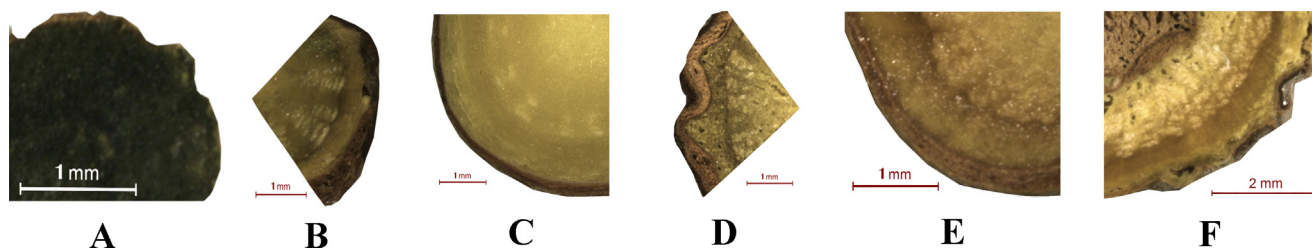


Fig. 6 Optical images of *Scutellariae Amoenae Radix* and *Scutellariae Radix*. Samples of *Scutellariae Amoenae Radix* were collected from Chuxiong, Yunnan (A) and Dali, Yunnan (B). Samples of *Scutellariae Radix* was collected from Hebei (C), Shanxi (D), Shandong (E) and Neimenggu (F).

capable of supporting the differentiation of SAR and SR. According to the distribution patterns of chemicals in SAR and SR, extracted mass images were divided into four groups. Different distribution patterns of phytochemicals in SAR and SR not only provided support for the quick differentiation of two species, but also brought new thoughts on the exploration of plant anatomy and plant physiology.

Constituents belonging to Pattern 1 were found to show an especially high intensity in the corks of SR and SAR. In plant anatomy, the cork usually referred to an outer protective tissue of roots, and was included in the periderm structure (Charles, 2010). Parenchyma cells in secondary phloem exhibit meristematic ability and form the phellogen (cork cambium). Con-

tinuous differentiation of phellogen brings about the formation of phellogen and phellem (cork). Subsequently, the first periderm is constructed (Boher et al., 2018). Abnormal structures such as interxylary cork and rhytidome may also occur during cork development. Rhytidome is composed of successively formed periderms and in-between tissues (Li et al., 2018). When rhytidome structure was formed, parenchyma cells in the deeper tissue of secondary phloem recover the capability of meristems, producing a new periderm. Finally, an anomalous structure of plant is developed (Han et al., 2021). Aside from rhytidome, interxylary cork is also an anomalous structure of root. At the beginning of interxylary cork development, some xylem vessels are gradually filled with tylosis or

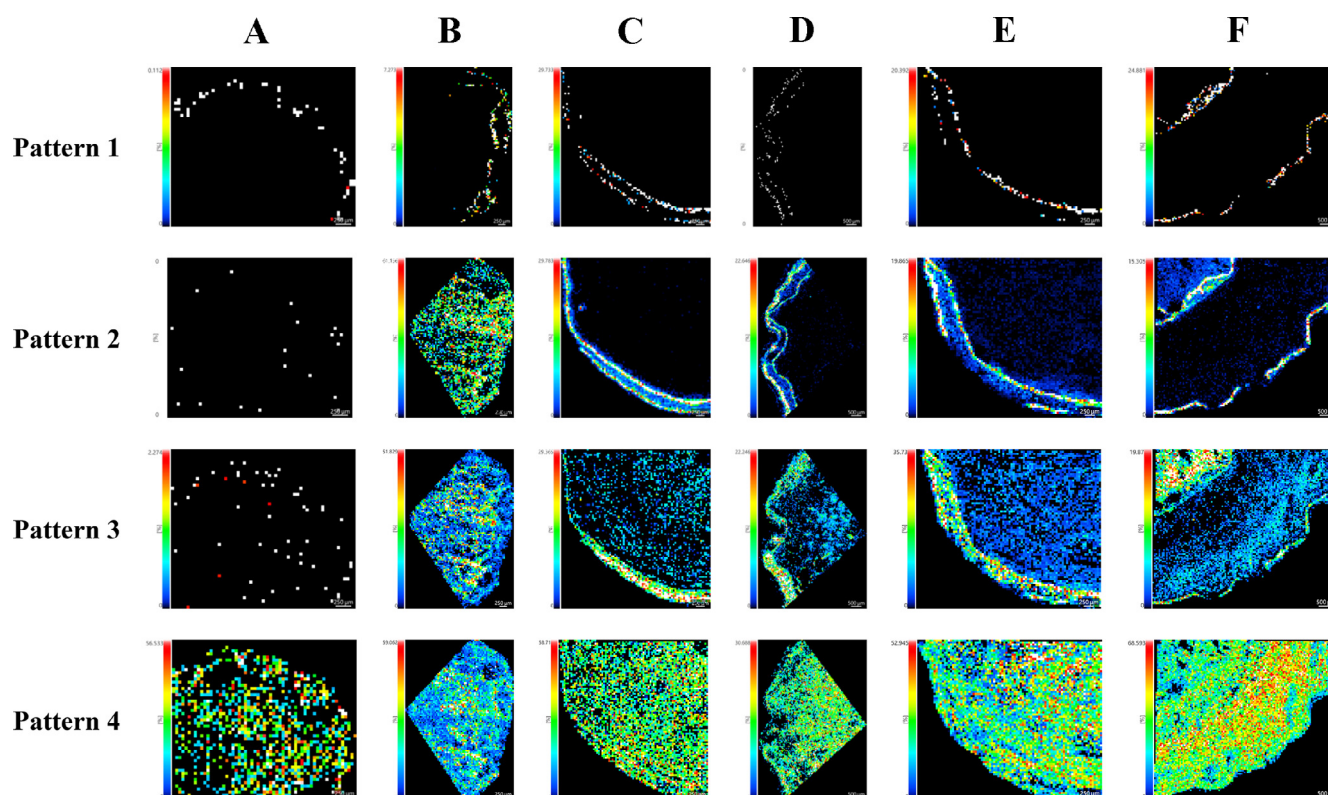


Fig. 7 Mass images representing different distribution patterns of phytochemicals in *Scutellariae Radix* and *Scutellariae Amoena Radix*. Representative mass images of Pattern 1, Pattern 2, Pattern 3 and Pattern 4 were extracted at m/z 433.3448 (unknown compound), m/z 413.0631 (identified as skullcapflavone II and/or its isomers), m/z 339.0265 (identified as scutevulin and/or its isomers) and m/z 303.0473 (identified as viscidulin I and/or its isomers) respectively. Samples of *Scutellariae Amoena Radix* were collected from Chuxiong, Yunnan (A) and Dali, Yunnan (B). Samples of *Scutellariae Radix* was collected from Hebei (C), Shanxi (D), Shandong (E) and Neimenggu (F).

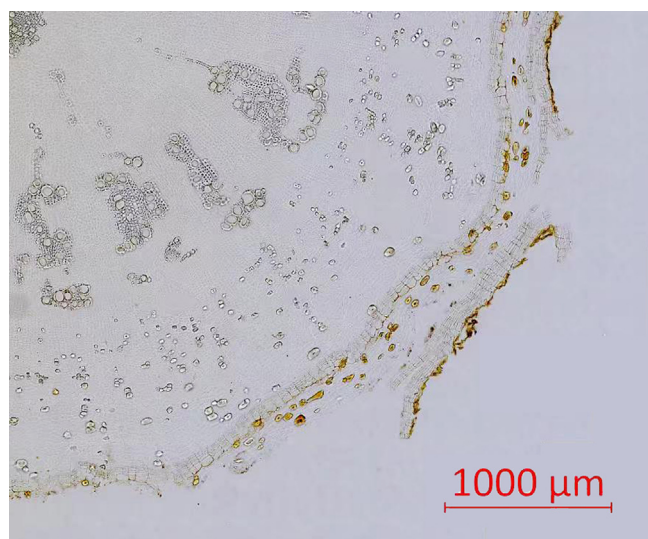


Fig. 8 A representative scanning image of a root sample containing rhytidome structure. The image was taken by Zeiss Axio Scan.Z1 automatic digital slide scanning system.

other substances. Soon, the tylosis begins to appear in parenchyma cells adjacent to these abnormal vessels. Then, nor-

mal parenchyma cells around the abnormal tissues regain their meristematic ability, forming a new phellogen in the phloem area. As the phellogen grows in a tangential direction, a cork layer is developed inwards. After that, healthy tissues were separated from the abnormal parenchyma cells and vessels by the interxylary cork (Wang et al., 2020). As was shown in Fig. 7, phytochemicals belonging to Pattern 1 were found to show an especially high intensity in the cork regions of SAR and SR. Interestingly, in Sample B-E, chemicals of Pattern 1 presented high abundance in the form of successive curves along the edge of root sections. The duplicated signals indicated that a repetition of certain structure emerged during root development. By conducting digital scanning of root sections, doubled corks were found in these samples. A typical microscopic image of the abnormal structure was displayed in Fig. 8. According to botanical knowledge, this special structure could be possibly assigned as rhytidome. Apart from rhytidome, interxylary cork was also found in one of the analyzed samples. In Sample F collected from Neimenggu, the high intensity of signals showed presence not only in the outer cork, but also around the border of interxylary cork. While the formation of interxylary cork in SR has been reported in many literatures, the presence of rhytidome in SR was seldom reported. Our findings suggested that MSI was capable of offering intuitive clues for deeper exploration of plant structures.

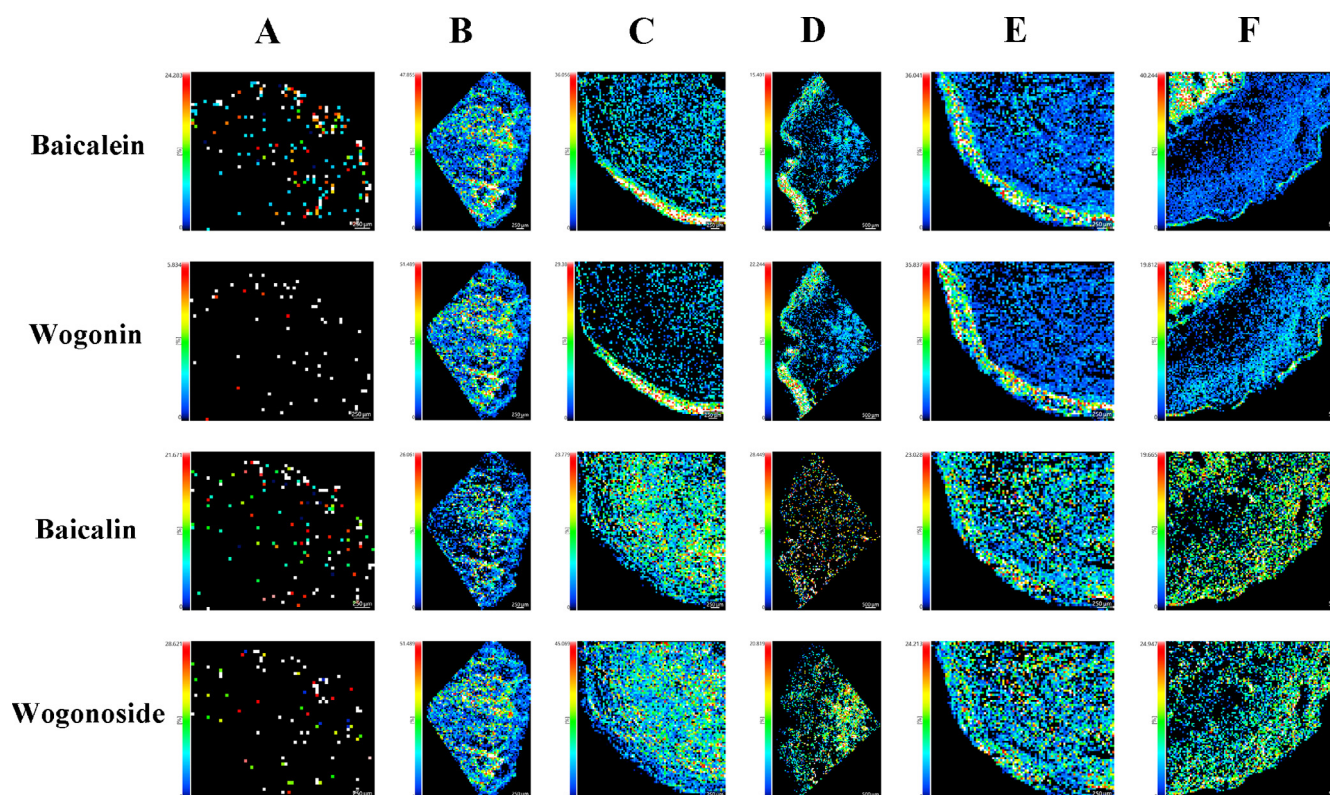


Fig. 9 Visualization of four major flavonoids in *Scutellariae Radix* and *Scutellariae Amoena Radix*. The potassium adducts of baicalein, wogonin, baicalin and wogonoside were extracted at m/z 309.0160, m/z 323.0309, m/z 485.0478 and m/z 499.0630 respectively. Samples of *Scutellariae Amoena Radix* were collected from Chuxiong, Yunnan (A) and Dali, Yunnan (B). Samples of *Scutellariae Radix* was collected from Hebei (C), Shanxi (D), Shandong (E) and Neimenggu (F).

Natural components falling into the categories of Pattern 2 showed different spatial localization features in SR and SAR. In SR, these chemicals were found to exhibit especially strong intensity along the corks of interxylary cork or rhytidome. However, in SAR, such metabolites presented no preferential occurrence in cork regions. The localization features of these phytochemicals could be utilized to differentiate SR from SAR.

Mass images of Pattern 3 elucidated that quite a few metabolites were abundantly stored in the dead phloem of rhytidome and the dead xylem of interxylary cork. Nevertheless, in the transverse sections of SAR, components of Pattern 3 were not found to exhibit especially high intensity in dead phloem surrounded by subsequent corks of rhytidome or dead xylem encircled by interxylary cork. The above phenomenon could also be employed to distinguish between SAR and SR.

Conventional analytical tools such as LC-MS, gas chromatography coupled with mass spectrometry (GC-MS) and high performance liquid chromatography (HPLC) were capable of unveiling the chemical composition of a plant sample. However, these conventional methods lacked the ability to provide spatial information of detected compounds. When conventional analytical methods were applied to elucidate the material basis of an herb, plant materials were usually pulverized into powder before the extraction of pharmaceutical components. During the homogenization process, spatial information of natural compounds was lost. The employment of MSI avoided the drawback of conventional analytical methods. Without any homogenization or extraction procedure,

natural compounds in root tissues of medicinal plants were directly mapped out. Based on the spatial information uncovered by MSI, a quick method for the differentiation of SR and SAR was established. As mentioned above, though compounds belonging to Pattern 2 and Pattern 3 showed existence in both species, MSI was still able to achieve the distinguishment of SR and SAR according to distribution features of chemicals within root tissues. In other words, MSI provided a new dimension for the comprehension of natural compounds within medicinal plants, and made up for the shortage of classic analytical tools.

4.3. On-tissue tandem mass spectrometry analysis

As stated before, the visualization of a target compound may be interfered by its possible isomers. In order to make a more precise observation of major flavonoids within SR samples, on-tissue tandem mass spectrometry analysis was carried out using MALDI-Q-TOF-MS. Protonated molecules of baicalein, wogonin, baicalin and wogonoside, together with the possible isomers of each flavonoid, were directly dissociated from the surface of roots sections. The reference standards of interest flavonoids were also analyzed using MALDI-Q-TOF-MS to provide referential information.

Norwogonin, apigenin and 2'-hydroxychrysin were the constitutional isomers of baicalein (Tomimori et al., 1984; Popova et al., 1973; Ma et al., 2013). Both baicalein and norwogonin were trihydroxylated on A ring. For apigenin and 2'-hydroxychrysin, two hydroxyl groups were distributed on A

ring, and another one on B ring. When cleavage of C—C bond at position 1/3 of flavonoids was triggered, different hydroxylated positions on A ring and B ring of flavonoid skeleton led to the formation of different $^{1,3}A^+$ fragments. Baicalein and norwogonin produced $^{1,3}A^+$ ion at m/z 169.0137, while apigenin and 2'-hydroxychrysin produced $^{1,3}A^+$ ion at m/z 153.0188. On-tissue dissociation of the precursor ion at m/z 271.0601 brought about the presence of fragment ions at m/z 169.0110, providing evidence for the existence of baicalein and norwogonin. Since baicalein and norwogonin had very similar chemical structure as well as fragmentation patterns, results supplied by tandem mass spectrometry were not sufficient enough to tell baicalein from norwogonin. The characteristic fragment of apigenin and 2'-hydroxychrysin, was not observed at m/z 153.0188. Therefore, apigenin and 2'-hydroxychrysin were likely to be absent from the chemical composition of analyzed SR sample. In conclusion, the mass image extracted at m/z 271.0601 (baicalein, $[M + H]^+$) was possibly a combined result of baicalein and norwogonin. It was stated in a previous article that norwogonin in SR presented much lower content compared to baicalein (Yan et al., 2014), the distribution of baicalein should be considered as a dominant participant in the mass image extracted at m/z 271.0601. In other words, the spatial distribution of baicalein uncovered by MSI was still considered a reliable result.

In the same manner, the fragmentation pattern of wogonin and its isomers was investigated. Oroxylin A, 5,6-dihydroxy-7-methoxyflavone and wogonin were flavonoids of similar structure, with a methoxy group and two hydroxyl groups locating on different positions of A ring. The structure of genkwanin was quite different from the three flavonoids mentioned above, two hydroxyl groups were separately distributed on A ring and B ring, and the methoxy group were distributed on A ring (Li et al., 2010). The $(^{1,3}A^+ - CH_3)$ ion of wogonin, oroxylin A and 5, 6-dihydroxy-7-methoxyflavone were observed at m/z 168.0053, whereas the diagnostic fragments of genkwanin, $(^{1,3}A^+ - CH_3 - CO)$ and $(^{1,3}A^+ - CH_3)$, were not detected.

Reported isomers of baicalin were norwogonin-7-*O*- β -*D*-glucuronide and apigenin-7-*O*- β -*D*-glucuronide (Ji et al., 2015; Ishimaru et al., 1995; Cha et al., 2006). The isomeric glycoside of wogonoside was oroxylin A-7-*O*- β -*D*-glucuronide (Ishimaru et al., 1995; Zhang et al. 1997). Characteristic fragments of flavonoid glucuronides were readily detected after the loss of glucuronic acid. Nevertheless, tandem mass spectrometry analysis carried out using MALDI-Q-TOF-MS was still unable to separate glucuronides from their isomers.

Overall, by performing tandem mass spectrometry, diagnostic fragments of protonated baicalein, wogonin, baicalin and wogonoside were successfully detected in the tandem mass spectra of SR. In the meantime, characteristic fragments of some possible isomers were not observed in tandem mass results, thus the existence of these possible isomers was rejected. Additionally, though the in situ dissociation of natural compounds could be achieved using tandem mass imaging, the intensity of produced fragments was not strong enough to construct ion images of high quality. At last, it was still a difficult task to distinguish between isomers sharing almost the same fragmentation patterns. More recently, ion mobility has been proven to be a successful method for the separation and detection of different structural isomers (Kiss et al., 2011). Hopefully, the combination of ion mobility and MSI may enhance the detailed exploration of in situ metabolites.

4.4. Visualization of four major flavonoids in *Scutellariae Radix* and *Scutellariae Amoena Radix*

Baicalein, wogonin, baicalin and wogonoside are four pharmaceutically important flavonoids in SR and SAR. As illustrated in Fig. 9, baicalein and wogonin were widely distributed in the whole transverse section of SAR, while in SR, an extremely high intensity was found in the dead phloem surrounded by subsequently formed corks of rhytidome or dead xlem encircled by interxylary cork.

The development of rhytidome and interxylary cork had a close connection with dead tissues. A previous literature stated that baicalein had close relationship with the programmed cell death of plants (Hirunuma et al., 2011). Now that both baicalein and wogonin were observed to present high content in dead phloem and xylem, it was reasonable to assume that wogonin was also an important metabolite associated with programmed cell death. Besides, it was widely acknowledged that flavonoids played a role in plant resistance against pathogenic bacteria and fungi (Mierziak et al., 2014). Therefore, the phenomena that wogonin and baicalein showed preferential accumulation along the edge of root sections provided validation for the plant defense function of endogenous flavones. Taken together, the application of MSI assisted in the exploration of physiological function of natural compounds.

Furthermore, accumulation sites of wogonin and baicalein uncovered by MSI could serve as a guidance for the high-efficiency extraction of major components from SR. Firstly, since rhytidome and interxylary cork were secondary structures that tended to appear in older roots, when selecting raw materials for the extraction of baicalein or wogonin, SR at older ages should be a better choice. Secondly, region-specific extraction could be utilized to arouse the efficiency of extraction. In Chinese Pharmacopoeia, before the clinical application of SR, it was required that the coarse bark of roots be removed (Chinese Pharmacopoeia Commission, 2020). However, MSI results suggested that high contents of wogonin and baicalein were distributed at the outer cork. Consequently, it was worth reconsidering whether the outer bark of SR should be removed during therapeutic application.

For the distribution of wogonoside and baicalin, no apparent accumulation in specific areas of roots was observed. The localization of two glucuronides presented a quite uniform distribution within the root tissues. Baicalin and wogonoside were the downstream product of baicalein and wogonin during the biosynthetic process. The wide distribution of two glucuronides indicated that enzymes which transformed free aglycones into corresponding glucuronides were also widely expressed in the root.

Based on the spatial distribution of baicalein, wogonin and their glucuronides, it was possible to hypothesize that when cell death was triggered, the activities of glucosyltransferase in dying tissues might sharply decrease. Meanwhile, the enzymes in living tissues were still capable of transforming aglycones into glucuronides. Therefore, abnormal xylem and parenchyma cells in the interxylary cork, as well as dead phloem tissues locating in successively formed periderms of rhytidome, appeared especially higher abundance of wogonin and baicalein. The other hypothesis may also explain why different spatial localization modes occurred between free flavonoids and their glucuronides. When cells were undergoing

apoptosis process, enzymes responsible for hydrolyzing baicalin and wogonoside into their aglycones were activated, leading to increased contents of baicalein and wogonin in dying tissues. It was demonstrated in an earlier research that baicalein was a stress inducible metabolite which was generally maintained at a quite low level in the roots of SR, whereas baicalin was abundantly stored as a precursor for the future release of baicalein. When plant tissues were wounded, hydrolysis of baicalin was triggered, giving rise to a higher level of baicalein in plant cells. It was found out that baicalein was able to translocate into the nucleus and then induce cell apoptosis through DNA oxidation, whereas its glucuronide, the baicalin, lacked the ability to move into the nucleus (Hirunuma et al., 2011). As a result, baicalein was more likely to accumulate in dead phloem or dead xylem of SR, while baicalin was evenly distributed in other areas. The transformation between wogonin and wogonoside may follow the same regulation as baicalein and baicalin. The two hypotheses stated above were not contradictory, one involving the consumption of baicalein and wogonin in living tissues and the other the hydrolyzation of baicalin and wogonoside in dying tissues, both contributed to a relatively higher abundance of wogonin and baicalein in dead tissues.

5. Conclusions

Visualization of phytochemicals in *Scutellariae Amoena Radix* and *Scutellariae Radix* were readily achieved using microscopic MSI. Distribution modes of natural compounds within two kinds of medicinal plants were divided into four groups. Quite a number of plant metabolites were found to distribute differently in SAR and SR. The results indicated that microscopic MSI was a potential tool for the quick differentiation of phylogenetically similar species. Moreover, spatial information of pharmaceutically important components provided new perspectives for the exploration of medicinal plants.

It was also feasible to carry out on-tissue tandem mass spectrometry analysis using the MALDI-Q-TOF-MS. Four important flavonoids, including baicalein, wogonin, baicalin and wogonoside, were directly dissociated from the transverse sections of SR. Fragments of flavonoids in native tissues matched with the characteristic ions generated from reference standards.

In the future, it would be an interesting and meaningful work to identify the unknown phytochemicals that presented different localization modes in SAR and SR. Besides, the combination of MSI with ion mobility could be employed to clarify the specific localization of target compounds from possible isomers.

Author Contributions

Lieyan Huang and Lixing Nie designed and performed the experiments, analyzed the data, and wrote the manuscript. Jing Dong, Lingwen Yao and Zhong Dai assisted in performing the experiments. Shuai Kang collected and authenticated the medicinal materials of *Scutellariae Radix* and *Scutellariae Amoena Radix*. Feng Wei and Shuangcheng Ma revised the manuscript. All authors read and approved the final manuscript.

Declaration of Competing Interest

The authors declare that they have no known competing financial interests or personal relationships that could have appeared to influence the work reported in this paper.

References

- Bjarnholt, N., Li, B., D'Alvise, J., Janfelt, C., 2014. Mass spectrometry imaging of plant metabolites-principles and possibilities. *Nat. Prod. Rep.* <https://doi.org/10.1039/c3np70100j>.
- Boher, P., Soler, M., Sánchez, A., Hoede, C., Noirot, C., Paiva, J.A.P., Serra, O., Figueras, M., 2018. A comparative transcriptomic approach to understanding the formation of cork. *Plant Mol. Biol.* 96, 103–118. <https://doi.org/10.1007/s11103-017-0682-9>.
- Cha, J.H., Kim, H.W., Kim, S., Jung, S.H., Whang, W.K., 2006. Antioxidant and anti-allergic activity of compounds from the aerial parts of *Scutellaria baicalensis* Georgi. *J. Pharm. Soc. Korea.* 50, 136–143.
- Charles, B.B., 2010. *An Introduction to Plant Structure and Development Plant Anatomy for the Twenty-First Century*. Cambridge, UK.
- Chinese Pharmacopoeia Commission, 2020. *Pharmacopoeia of People's Republic of China*, first ed. Beijing, China, 2020
- Chung, H., Huang, P., Chen, C.L., Lee, C., Hsu, C.C., 2022. Next-generation pathology practices with mass spectrometry imaging. *Mass Spectrom. Rev.* e21795, 1–20. <https://doi.org/10.1002/mas.21795>.
- Cuyckens, F., Claeys, M., 2004. Mass spectrometry in the structural analysis of flavonoids. *J. Mass Spectrom.* 39, 1–15. <https://doi.org/10.1002/jms.585>.
- Deng, Y.T., Liao, Q.F., Li, S.H., Bi, K.S., Pan, B.Y., Xie, Z.Y., 2008. Simultaneous determination of berberine, palmatine and jatrorrhizine by liquid chromatography–tandem mass spectrometry in rat plasma and its application in a pharmacokinetic study after oral administration of coptis-evodia herb couple. *J. Chromatogr. B: Anal. Technol. Biomed. Life Sci.* 863, 195–205. <https://doi.org/10.1016/j.jchromb.2007.12.028>.
- Duan, S.Y., Li, X.Q., Yao, Z.H., Zhang, X.J., Yao, X.S., Yang, J., Qin, Z.F., 2022. Visual authentication of steroidal saponins in *Allium macrostemon* Bge. and *Allium chinense* G. Don using MALDI-TOF imaging mass spectrometry and their structure activity relationship. *Arabian J. Chem.* 104138, 1–14. <https://doi.org/10.1016/j.arabjc.2022.104138>.
- Feng, B., Zhang, J., Chang, C., Li, L., Li, M., Xiong, X., Guo, C., Tang, F., Bai, Y., Liu, H., 2014. Ambient mass spectrometry imaging: Plasma assisted laser desorption ionization mass spectrometry imaging and its applications. *Anal. Chem.* 86, 4164–4169. <https://doi.org/10.1021/ac403310k>.
- Freitas, J.R.L., Vendramini, P.H., Melo, J.O.F., Eberlin, M.N., Augusti, R., 2019. Assessing the spatial distribution of key flavonoids in *Mentha × piperita* Leaves: an application of desorption electrospray ionization mass spectrometry imaging (DESI-MSI). *J. Braz. Chem. Soc.* 30, 1437–1446. <https://doi.org/10.21577/0103-5053.20190039>.
- Han, S., Kim, H.M., Lee, J.M., Mok, S.Y., Lee, S., 2010. Isolation and identification of polymethoxyflavones from the hybrid citrus, hallabong. *J. Agric. Food Chem.* 58, 9488–9491. <https://doi.org/10.1021/jf102730b>.
- Han, X., Zhou, Y., Ni, X., Chu, S., Cheng, M., Tan, L., Zha, L., Peng, H., 2021. Programmed cell death during the formation of rhytidome and interxylary cork in roots of *Astragalus membranaceus* (Leguminosae). *Microsc. Res. Tech.* 84, 1400–1413. <https://doi.org/10.1002/jemt.23696>.
- Hirunuma, M., Shoyama, Y., Sasaki, K., Sakamoto, S., Taura, F., Shoyama, Y., Tanaka, H., Morimoto, S., 2011. Flavone-catalyzed apoptosis in *Scutellaria baicalensis*. *Phytochemistry* 72, 752–760. <https://doi.org/10.1016/j.phytochem.2011.02.009>.
- Huang, H.Z., Tan, P., Li, M.Q., Tan, Q.C., Gao, J.H., Bao, X.M., Fan, S.H., M, T.G., Mao, W.M., Lin, F., Han, L., Zhang, D.K., Lin, J.Z., 2022a. Quality analysis combined with mass spectrometry imaging reveal the difference between wild and cultivated *Phyllanthus emblica* Linn.: From chemical composition to molecular

- mechanism. *Arabian J. Chem.* 103790, 1–17. <https://doi.org/10.1016/j.arabjc.2022.103790>
- Huang, L., Nie, L., Dai, Z., Dong, J., Jia, X., Yang, X., Yao, L., Ma, S.C., 2022b. The application of mass spectrometry imaging in traditional Chinese medicine: a review. *Chinese Med. (United Kingdom)* 17, 1–20. <https://doi.org/10.1186/s13020-022-00586-8>.
- Husain, M., Husain, S., Ali, J., 2020. Differential distribution of characteristic constituents in root, stem and leaf tissues of *Salvia miltiorrhiza* using MALDI mass spectrometry imaging. *Diam. Relat. Mater.* 146, 108139.
- Huynh, D.L., Sharma, N., Kumar Singh, A., Singh Sodhi, S., ZHANG, J.J., Mongre, R.K., Ghosh, M., Kim, N., Ho Park, Y., Kee Jeong, D., 2017. Anti-tumor activity of wogonin, an extract from *Scutellaria baicalensis*, through regulating different signaling pathways. *Chin. J. Nat. Med.* 15, 15–40. [https://doi.org/10.1016/S1875-5364\(17\)30005-5](https://doi.org/10.1016/S1875-5364(17)30005-5)
- Ishimaru, K., Nishikawa, K., Omoto, T., Asai, I., Yoshihira, K., Shimomura, K., 1995. Two flavone 2'-glucosides from *Scutellaria baicalensis*. *Phytochemistry*. 40, 279–281. [https://doi.org/10.1016/0031-9422\(95\)00200-Q](https://doi.org/10.1016/0031-9422(95)00200-Q).
- Ji, S., Li, R., Wang, Q., Miao, W.J., Li, Z.W., Si, L.L., Qiao, X., Yu, S. W., Zhou, D.M., Ye, M., 2015. Anti-H1N1 virus, cytotoxic and Nrf2 activation activities of chemical constituents from *Scutellaria baicalensis*. *J. Ethnopharmacol.* 176, 475–484. <https://doi.org/10.1016/j.jep.2015.11.018>.
- Karimov, A.M., Botirov, E.K., 2017. Structural diversity and state of knowledge of flavonoids of the *Scutellaria* L. Genus. *Russ. J. Bioorganic Chem.* 43, 691–711. <https://doi.org/10.1134/S1068162017070068>.
- Kenney, K.B., Wring, S.A., Carr, R.M., Wells, G.N., Dunn, J.A., 2000. Simultaneous determination of zidovudine and lamivudine in human serum using hplc with tandem mass spectrometry. *J. Pharm. Biomed. Anal.* 22, 967–983. [https://doi.org/10.1016/S0731-7085\(00\)00248-x](https://doi.org/10.1016/S0731-7085(00)00248-x).
- Kim, J.K., Kim, Y.S., Kim, Y.J., Uddin, M.R., Kim, Y.B., Kim, H.H., 2014. Comparative analysis of flavonoids and polar metabolites from hairy roots of *Scutellaria baicalensis* and *Scutellaria lateriflora*. *World J. Microbiol. Biotechnol.* 30, 887–892. <https://doi.org/10.1007/s11274-013-1498-7>.
- Kiss, A., Heeren, R.M.A., 2011. Size, weight and position: ion mobility spectrometry and imaging MS combined. *Anal. Bioanal. Chem.* 399, 2623–2634. <https://doi.org/10.1007/s00216-010-4644-1>.
- Kubo, M., Kimura, Y., Odani, T., Tani, T., Namba, K., 1981. Studies on *Scutellariae Radix*. Part II: the antibacterial substance. *Planta Medica*. 43, 194–201. <https://doi.org/10.1055/s-2007-971499>.
- Kuo, T.H., Huang, H.C., Hsu, C.C., 2019. Mass spectrometry imaging guided molecular networking to expedite discovery and structural analysis of agarwood natural products. *Anal. Chim. Acta* 1080, 95–103. <https://doi.org/10.1016/j.aca.2019.05.070>.
- Li, L.Z., Gao, P.Y., Peng, Y., Wang, L.H., Song, S.J., 2010. A novel Daphnane-type Diterpene from the flower bud of *Daphne Genkwa*. *Chem. Nat. Compd.* 46, 380–382.
- Li, R., Yin, M., Yang, M., Chu, S., Han, X., Wang, M., Peng, H., 2018. Developmental anatomy of anomalous structure and classification of commercial specifications and grades of the astragalus membranaceus Var. *Mongholicus*. *Microsc. Res. Tech.* 81, 1165–1172.
- Lin, W., Liu, S., Wu, B., 2013. Structural identification of chemical constituents from *Scutellaria baicalensis* by HPLC-ESI-MS/MS and NMR spectroscopy. *Asian J Chem.* 25, 3799–3805. <https://doi.org/10.14233/ajchem.2013.13788>.
- Ling, X., Fei, Z., 2016. Research on the differentiation of *Scutellaria baicalensis* Georgi and *Scutellaria amoena* C.H.Wright. *J. Chinese Med. Mater.* 39, 2412–2416.
- Liu, H., Dong, Y., Gao, Y., Du, Z., Wang, Y., Cheng, P., Chen, A., Huang, H., 2016. The fascinating effects of baicalin on cancer: a review. *Int. J. Mol. Sci.* 17, 1–18. <https://doi.org/10.3390/ijms17101681>.
- Liu, Y.X., Liu, Z.G., Su, L., Yang, R.P., Hao, D.F., Pei, Y.H., 2009. Chemical constituents from *Scutellaria baicalensis* Georgi. *Chin. J. Med. Chem.* 19, 59–62.
- Liu, G., Ma, J., Chen, Y., Tian, Q., Shen, Y., Wang, X., Chen, B., Yao, S., 2009. Investigation of flavonoid profile of *Scutellaria baicalensis* Georgi by high performance liquid chromatography with diode array detection and electrospray ion trap mass spectrometry. *J. Chromatogr. A* 1216, 4809–4814. <https://doi.org/10.1016/j.chroma.2009.04.021>.
- Liu, G.Z., Rajesh, N., Wang, X.S., Zhang, M.S., Wu, Q., Li, S.J., Chen, B., Yao, S.Z., 2011. Identification of flavonoids in the stems and leaves of *Scutellaria baicalensis* Georgi. *J. Chromatogr. B, Anal Technol Biomed Life Sci.* 879, 1023–1028. <https://doi.org/10.1016/j.jchromb.2011.02.050>.
- Liu, Z.B., Sun, C.P., Xu, J.X., Morisseau, C., Hammock, B.D., Qiu, F., 2019. Phytochemical constituents from *Scutellaria baicalensis* in soluble epoxide hydrolase inhibition: Kinetics and interaction mechanism merged with simulations. *Int. J. Biol. Macromol.* 133, 1187–1193. <https://doi.org/10.1016/j.ijbiomac.2019.04.055>.
- Liu, D.W., Yan, G.L., Yuan, F., Liu, S.M., 2012. Utility of uplc-esi-tof/ms for rapid analysis of the constituents in *scutellariae radix*. *Chin. J. Inf. Tradit. Chin. Med.* 29, 20–24. <https://doi.org/10.3969/j.issn.1002-2406.2012.04.009>.
- Long, H.L., Xu, G.Y., Deng, A.J., Li, Z.H., Ma, L., Lu, Y., Zhang, Z. H., Wu, F., Qin, H.L., 2015. Two new flavonoids from the roots of *Scutellaria baicalensis*. *J. Asian Nat. Prod. Res.* 17, 756–760. <https://doi.org/10.1080/10286020.2014.999048>.
- Ma, J.L., 2013. Study on chemical constituents from stems and leaves of *Scutellaria baicalensis*. *Chin. J. Exp. Trad. Med. Formulae* 19, 147–149. <https://doi.org/10.11653/zgsyfyjzz2013070147>.
- Ma, Y.L., Li, Q.M., Van Den Heuvel, H., Claeys, M., 1997. Characterization of flavone and flavonol aglycones by collision-induced dissociation tandem mass spectrometry. *Rapid Commun. Mass Spectrom.* 11, 1357–1364.
- Marques, J.V., Dalisay, D.S., Yang, H., Lee, C., Davin, L.B., Lewis, N.G., 2014. A multi-omics strategy resolves the elusive nature of alkaloids in *Podophyllum* species. *Mol. Biosyst.* 10, 2838–2849. <https://doi.org/10.1039/c4mb00403e>.
- McDonnell, L.A., Angel, P.M., Lou, S., Drake, R.R., 2017. Mass spectrometry imaging in cancer research: future perspectives. *Adv. Cancer Res.* 134, 283–290. <https://doi.org/10.1016/bs.acr.2016.11.010>.
- Medical Products Administration of Yunnan Province, 2005. *Yunnan Standard of Chinese Materia Medica*. first ed. Kunming, China
- Mierziak, J., Kostyn, K., Kulma, A., 2014. Flavonoids as important molecules of plant interactions with the environment. *Molecules* 19, 16240–16265.
- Miyaichi, Y., Tomimori, T., 1994. Studies on the constituents of *Scutellaria* species XVI: phenol glycosides of the root of *Scutellaria baicalensis* Georgi. *J. Nat. Med.* 48, 215–218.
- Miyaichi, Y., Tomimori, T., 1995. Studies on the constituents of *Scutellaria* Species XVII: phenol glycosides of the root of *Scutellaria baicalensis* Georgi. *J. Nat. Med.* 49, 350–353.
- Nagai, T., Miyaichi, Y., Tomimori, T., Yamada, H., 1998. Inhibition of mouse liver sialidase by plant flavonoids. *Biochem. Biophys. Res. Commun.* 163, 25–31.
- Nie, L., Dong, J., Huang, L., Qian, X., Lian, C., Kang, S., 2021. Microscopic mass spectrometry imaging reveals the distribution of phytochemicals in the dried root of *isatis tinctoria*. *Front. Pharmacol.* 12. <https://doi.org/10.3389/fphar.2021.685575>.
- Nishikawa, K., Furukawa, H., Fujioka, T., Fujii, H., Mihashi, K., Shimomura, K., Ishimaru, K., 1999. Flavone production in transformed root cultures of *Scutellaria baicalensis* Georgi. *Phytochemistry* 52, 885–890. [https://doi.org/10.1016/S0031-9422\(99\)00306-4](https://doi.org/10.1016/S0031-9422(99)00306-4).
- Popova, T.P., Litvinenko, V.I., Kovalev, I.P., 1973. Flavones of the roots of *Scutellaria baicalensis*. *Chem. Nat. Compd.* 9, 699–702. <https://doi.org/10.1007/BF00565789>.

- Pramanik, S.K., Suja, F.B., Zain, S., Pramanik, B.K., 2019. A spatially-resolved approach to visualize the distribution and biosynthesis of flavones in *Scutellaria baicalensis* Georgi. *Biore-sour. Technol. Rep.* 179, 100310.
- Qiao, X., Li, R., Song, W., Miao, W.J., Liu, J., Chen, H.B., Guo, D. A., Ye, M., 2016. A targeted strategy to analyze untargeted mass spectral data: rapid chemical profiling of *Scutellaria baicalensis* using ultra-high performance liquid chromatography coupled with hybrid quadrupole orbitrap mass spectrometry and key ion filtering. *J. Chromatogr. A* 1441, 83–95. <https://doi.org/10.1016/j.chroma.2016.02.079>.
- Schulz, S., Becker, M., Groseclose, M.R., Schadt, S., Hopf, C., 2019. Advanced MALDI mass spectrometry imaging in pharmaceutical research and drug development. *Curr. Opin. Biotechnol.* 55, 51–59. <https://doi.org/10.1016/j.copbio.2018.08.003>.
- Sturtevant, D., Lee, Y.J., Chapman, K.D., 2015. Matrix Assisted Laser Desorption/Ionization-Mass Spectrometry Imaging (MALDI-MSI) for Direct Visualization of Plant Metabolites. *Curr. Opin. Biotechnol.* 37, 53–60. <https://doi.org/10.1016/j.copbio.2015.10.004>.
- Sun, Y., Zhao, Y., Wang, X., Zhao, L., Li, W., Ding, Y., Kong, L., Guo, Q., Lu, N., 2016. Wogonoside prevents colitis-associated colorectal carcinogenesis and colon cancer progression in inflammation-related microenvironment via inhibiting NF- κ B activation through PI3K/Akt pathway. *Oncotarget* 7, 34300–34315. <https://doi.org/10.18632/oncotarget.8815>.
- Syrjänen, K., Sipilä, J., Björk, H., 2000. The identification of dilignols from dehydrogenation mixtures of coniferyl alcohol and apocynol [4-(1-Hydroxyethyl)-2-methoxyphenol] by LC-ES-MS/MS. *J. Agric. Food Chem.* 48, 5211–5215. <https://doi.org/10.1021/jf000598u>.
- Takagi, S., Yamaki, M., Inoue, K., 1980. Studies on the water-soluble constituents of the roots of *Scutellaria baicalensis* Georgi (wogon). *J. Pharm. Soc. Jpn.* 100, 1220–1224. https://doi.org/10.1248/yakushi1947.100.12_1220.
- Takagi, S., Yamaki, M., Inoue, K., 1981. Flavone Di C-glycosides from *Scutellaria baicalensis*. *Phytochemistry* 20, 2443. [https://doi.org/10.1016/S0031-9422\(00\)82692-8](https://doi.org/10.1016/S0031-9422(00)82692-8).
- Takido, M., Aimi, M., Yamanouchi, S., Yasukawa, K., Torii, H., Takahashi, S., 1976. Studies on the constituents in the water extracts of crude drugs. II. on the leaves of *Scutellaria baicalensis* Georgi. *J. Pharm. Soc. Jpn.* 96, 381–383. [https://doi.org/10.1002/\(SICI\)1097-0347\(199808\)20:5<411::AID-HED9>3.0.CO;2-0](https://doi.org/10.1002/(SICI)1097-0347(199808)20:5<411::AID-HED9>3.0.CO;2-0).
- Takido, M., Yasukawa, K., Matsuura, S., Inuma, M., 1979. On the revised structure of skullcapflavone I, a flavone compound in the roots of *Scutellaria baicalensis* Georgi (wogon). *J. Pharm. Soc. Jpn.* 99, 443–444.
- Tao, Y., Zhan, S., Wang, Y., Zhou, G., Liang, H., Chen, X., Shen, H., 2018. Baicalin, the major component of traditional Chinese medicine *Scutellaria baicalensis* induces colon cancer cell apoptosis through inhibition of oncomiRNAs. *Sci. Rep.* 8, 1–11. <https://doi.org/10.1038/s41598-018-32734-2>.
- Tomimori, T., Miyaichi, Y., Kizu, H., 1981. On the flavonoid constituents from the roots of *Scutellaria baicalensis* Georgi. *J. Pharm. Soc. Jpn.* 101, 899. https://doi.org/10.1248/yakushi1947.102.4_388.
- Tomimori, T., Miyaichi, Y., Imoto, Y., 1983. Studies on the constituents of *Scutellaria* species II. On the flavonoid constituents of the roots of *Scutellaria baicalensis* Georgi. *J. Pharm. Soc. Jpn.* 103, 607–611. https://doi.org/10.1248/yakushi1947.103.6_607.
- Tomimori, T., Miyaichi, Y., Imoto, Y., Kizu, H., Tanabe, Y., 1984. Studies on the constituents of *Scutellaria* species. On the flavonoid constituents of the root of *Scutellaria baicalensis* Georgi. *J. Pharm. Soc. Jpn.* 104, 524–528. https://doi.org/10.1248/yakushi1947.104.5_524.
- Tomimori, T., Miyaichi, Y., Imoto, Y., 1984. Studies on the constituents of *Scutellaria* species IV on the flavonoid constituents of the root of *Scutellaria baicalensis* Georgi. *J. Pharm. Soc. Jpn.* 104, 529. https://doi.org/10.1248/yakushi1947.105.2_148.
- Wang, Y., Guo, Z., Jin, Y., Zhang, X., Li, W., Liang, X., 2009. Selective enrichment with “click oligo (ethylene glycol)” column and TOF-MS characterization of simple phenylpropanoids in the fruits of *Forsythia suspensa*. *J. Sep. Sci.* 32, 2958–2966.
- Wang, Z.L., Wang, S., Kuang, Y., Hu, Z.M., Qiao, X., Ye, M., 2018. A comprehensive review on phytochemistry, pharmacology, and flavonoid biosynthesis of *scutellaria baicalensis*. *Pharm. Biol.* 56, 465–484. <https://doi.org/10.1080/13880209.2018.1492620>.
- Wang, J., Yan, Y.G., Zhang, G., Peng, L., Chen, Y., 2020. The study on the formation and development of interxylary cork in roots of *Scutellaria baicalensis*. *Acta Bot. Boreali-Occident. Sin.* 40, 1672–1678. <https://doi.org/10.7606/j.issn.1000-4025.2020.10.1672>.
- Wang, H.W., Yin, Z.F., Li, H.B., Yuan, X.X., Yang, M.M., Zhao, G. Q., 2016. Chemical constituents from stems and leaves of *Scutellaria baicalensis*. *Chin. J. Exp. Trad. Med. Formulae* 22, 41–44. <https://doi.org/10.13422/j.cnki.syfjx.2016220041>.
- Wolfender, J.L., Waridel, P., Ndjoko, K., Hobby, K.R., Major, H.J., Hostettmann, K., 2000. Evaluation of Q-TOF-MS/MS and multiple stage IT-MSn for the dereplication of flavonoids and related compounds in crude plant extracts. *Analisis* 28, 895–906. <https://doi.org/10.1051/analisis:2000280895>.
- Xiao, L.H., Wang, H.Y., Song, S.J., 2003. The isolation and identification of chemical constituents of *Scutellaria amoena* C.H. Wright. *J. Shenyang Pharm. Univ.* 20, 181–183. <https://doi.org/10.3969/j.issn.1006-2858.2003.03.008>.
- Xiong, L.W., Zhao, H.W., Wang, Y., 2022. Study on phenolic acids of *Lonicerae Japonicae Flos* based on ultrahigh performance liquid chromatography-tandem mass spectrometry combined with multivariate statistical analysis. *J. Sep. Sci.* 45, 2239–2251. <https://doi.org/10.7501/j.issn.0253-2670.2015.04.006>.
- Xu, J.X., Ding, L.Q., Jiang, M.M., Qiu, F., 2016. Non-flavonoid constituents from the roots of *Scutellaria baicalensis* Georgi. *Chin. J. Med. Chem.* 26, 480–483. <https://doi.org/10.14142/j.cnki.cn21-1313/r.2016.06.007>.
- Yan, M., Xu, F.L., Xu, B., He, S.M., Mei, X.L., 2014. Content Determination of 5 kinds of flavonoid aglycone in *Scutellaria baicalensis* from different sources by RP-HPLC. *China Pharm.* 25, 1782–1784.
- Yang, D.P., Zhang, X.L., Pierre, J., Millet, J., 1999. Study on the volatile components in *Scutellaria baicalensis* Georgi. *Tradit. Chin. Drug Res. Clin. Pharmacol.* 4, 15. <https://doi.org/10.3321/j.issn:1003-9783.1999.04.015>.
- Zhang, Y.Y., Guo, Y.Z., Onda, M., Hashimoto, K., Ikeya, Y., Okada, M., Maruno, M., 1994. Four flavonoids from *Scutellaria baicalensis*. *Phytochemistry* 35, 511–514.
- Zhang, Y.Y., Guo, Y.Z., Ageta, H., Harigaya, Y., Onda, M., Hashimoto, K., Ikeya, Y., Okada, M., Maruno, M., 1997. A new flavone C-glycoside from *Scutellaria baicalensis*. *J. Chin. Pharm. Sci.* 6, 182–186.
- Zhang, L., Zhang, R.W., Li, Q., Lian, J.W., Liang, J., Chen, X.H., Bi, K.S., 2007. Development of the fingerprints for the quality evaluation of *Scutellariae Radix* by HPLC-DAD and LC-MS-MS. *Chromatographia* 66, 13–20. <https://doi.org/10.1365/s10337-007-0250-6>.
- Zhao, Q., Chen, X.Y., Martin, C., 2016. *Scutellaria baicalensis*, the golden herb from the garden of Chinese medicinal plants. *Sci. Bull.* 61, 1391–1398. <https://doi.org/10.1007/s11434-016-1136-5>.
- Zheng, H.Z., Dong, Z.H., Yu, J., 1998. Modern study and application of traditional Chinese medicine. Beijing, China.
- Zhou, Y., Hirotsani, M., Yoshikawa, T., Furuya, T., 1997. Flavonoids and phenylethanoids from hairy root cultures of *Scutellaria baicalensis*. *Phytochemistry* 44, 83–87. [https://doi.org/10.1016/S0031-9422\(96\)00443-8](https://doi.org/10.1016/S0031-9422(96)00443-8).
- Zhou, Z.H., Yang, C.R., 2000. Five new flavonoid glycosides in *Scutellaria amoena* C.H.Wright. *Plant Diversity Resour.* 22, 475–481. <https://doi.org/10.3969/j.issn.2095-0845.2000.04.017>.